Spring 2022

# Cycles or Repetitions: A Quantitative Analysis of Alluvial Bed Thicknesses

Kristopher D. Phillips
*Western Washington University*, krisp@smu.edu

**Cycles or Repetitions: A Quantitative Analysis of Alluvial Bed Thicknesses**

By

Kristopher D. Phillips

Accepted in Partial Completion
of the Requirements for the Degree
Master of Science

ADVISORY COMMITTEE

Dr. Brady Z. Foreman, Chair

Dr. Melissa Rice

Dr. Douglas Clark

GRADUATE SCHOOL

David L. Patrick, Dean

**Master's Thesis**

In presenting this thesis in partial fulfillment of the requirements for a master's degree at Western Washington University, I grant to Western Washington University the non-exclusive royalty-free right to archive, reproduce, distribute, and display the thesis in any and all forms, including electronic format, via any digital library mechanisms maintained by WWU.

I represent and warrant this is my original work, and does not infringe or violate any rights of others. I warrant that I have obtained written permissions from the owner of any third party copyrighted material included in these files.

I acknowledge that I retain ownership rights to the copyright of this work, including but not limited to the right to use all or part of this work in future works, such as articles or books.

Library users are granted permission for individual, research and non-commercial reproduction of this work for educational purposes only. Any further digital posting of this document requires specific permission from the author.

Any copying or publication of this thesis for commercial purposes, or for financial gain, is not allowed without my written permission.

Kristopher D. Phillips

May 4, 2022

# Cycles or Repetitions: A Quantitative Analysis of Alluvial Bed Thicknesses

A Thesis

Presented to

The Faculty of

Western Washington University

In Partial Fulfillment

Of the Requirements for the Degree

Master of Science

by

Kristopher D. Phillips

May 2022

## Abstract

Sedimentary strata display a range of repetitive patterns from interbedded lithofacies through recurring sequence stratigraphic systems tracts. Highly structured, large-scale patterns are commonly ascribed to cyclic allogenic forcings such as eustasy and climate. In contrast, autogenic processes are typically thought to impart stochastic noise or limited small-scale structure on stratigraphy. Recent studies indicate some autogenic processes in fluvial and fluvio-deltaic systems such as the large-scale compensational deposition (i.e., the tendency for a channel to occupy and fill topographic lows in a basin), can occur on spatiotemporal scales that may overlap with some allogenic forcings. These autogenic processes could impart deterministic, highly structured patterns in stratigraphy. Thus, assuming autogenic deposition is stochastic may lead to overinterpreting stratigraphic organization as externally driven. Herein I evalute this organization using two case studies.

Beds are the fundamental unit from which stratigraphic patterns are built, and here I evaluate bed thickness patterns within a purely autogenic experimental depositional system as well as in a field-scale basin potentially influenced by precession-scale orbital forcings (early Paleogene Willwood Formation, Bighorn Basin, Wyoming, USA). The purely autogenic experimental system (TDB-10-1) was created in the Sediment Dynamics Laboratory at Tulane University. In 67% of these synthetic stratigraphic sections, the spectral analysis identified statistically significant repetitions in bed thickness (at 99% confidence interval). However, the period of these cycles was not uniform, and in only 4% of cases was the identified period consistent with the known compensation timescale (222 minutes). The early Paleogene Willwood Formation data was recovered by the Bighorn Basin Coring Project in 2011. In the field study area, bed thicknesses with linearly interpolated ages from three cores were submitted to the same spectral analysis wherein cycles with periods of 3.5 kyrs, 3.7 kyrs and 15.0 kyrs were identified. These do not correspond to precession-scale (21 kyrs) variability previously identified by other researchers. The field and experimental results suggest noisy autogenic processes can produce spurious sub-Milankovitch cycles in stratigraphy, and that long-term autogenic compensational behavior is not cyclical. Moreover, experimental and field cases illustrate that it is possible to produce repetitive stratigraphy that does not predictably occur across the basin. These and other stratigraphic repetitions have been coined autocyclic in previous studies. I suggest the community restrict the

widely adopted term “cyclic” to those processes with regularity in the time doman across basin, and adopt “auto-repetitions” for local autogenic processes with irregularity in the time domain.

**Acknowledgements**

This research was possible through the funding provided by the Petroleum Research Fund New Undergraduate Investigator Grant (#57156 UNI-8 to Brady Z. Foreman) and the Western Washington University Department of Geology (Graduate Research Grant to Kristopher D. Phillips).

Thank you to Dick Giesecke for asking me about my research the first time I met you and the countless times you listened to me explain it after that. Thank you to Alina Holmes for sitting on Teams with me while I finally wrote down paragraphs that I had thought about for 3 years. Thank you to Rod Schaefer for firing me in the middle of a global pandemic so I could finally have the time to make this happen. Thank you to Whatcom Falls Park for providing a place to clear my head on all of those dark and rainy days. Thank you to the Graduate School for providing answers to all my questions and an extension to finish my thesis.

Thank you to my thesis committee for their valuable feedback that improved this project. Thank you Melissa Rice for providing a model for the teacher that I want to become. Thank you to Doug Clark for agreeing to jump on this committee on such short notice.

Thank you to the Bellingham and WWU community for welcoming and supporting me through some of the toughest moments of my life.

Thank you to Penelope Phillips for being an inspiration to do the hardest things. When I tell you that you can do anything, I mean it. Look, Daddy finished that big paper that took forever.

Thank you to Megan Giesecke for providing love, support, and encouragement when I had given up, but refused to admit it. I love you and am honored to call you my partner.

Finally, thank you to Brady Foreman. There is not another advisor in the world with the amount of patience and grace as you have shown me these last 5+ years. This thesis is truly a miracle and could not have happened without your wisdom and support. You were always there to support me; whether it was with a pint of Ben and Jerry's or permission to leave midyear and finish from Texas. I will never forget all that you have done for me. Thank you for allowing me to be your student.

## Table of Contents

Abstract ..... iv

Acknowledgements ..... vi

List of Figures and Tables ..... viii

1. Introduction ..... 1

2. Background ..... 7

    2.1 Stratigraphic Experiments & Compensation Timescale ..... 7

    2.2 Geologic Setting of the Bighorn Basin ..... 9

3. Materials and Methods ..... 12

    3.1 Stratigraphic Experiment ..... 12

    3.2 Bighorn Basin Core ..... 15

    3.3 Bed Thickness Distribution ..... 17

4. Results ..... 18

    4.1 Stratigraphic Experiment ..... 18

    4.2 Bighorn Basin ..... 18

    4.3 Bed Thickness Distribution ..... 19

5. Discussion ..... 20

    5.1 Statistical Distribution of Bed Thicknesses ..... 20

    5.2 Stratigraphic Experiment ..... 23

    5.3 Bighorn Basin Core ..... 25

    5.4 Inverse Problem ..... 28

6. Conclusions ..... 29

Works Cited ..... 32

## List of Figures and Tables


1. Figure 1: Experimental Setup Schematic.....43
2. Figure 2: Map of Field Study Area and Stratigraphic Columns of Cores.....44
3. Figure 3: Outcrop Photographs of the Willwood Formation, Bighorn Basin.....44
4. Figure 4: Nondimensionalized Discontinuous Time Series Plots for Cores.....45
5. Figure 5: Nondimensionalized Discontinuous Time Series Plots for Experimental.....46
6. Figure 6: Histogram Experimental Bed Thickness Cycles.....47
7. Figure 7: Log-log Plots of Bed Thickness Distributions for Cores and Experimental.....48
8. Table 1: Experimental Cycles Data.....49
9. Table 2: Trendline Equations and R-squared Values.....49

## 1. Introduction

Sedimentary processes and their resulting stratigraphy allow for reconstruction and understanding of paleo-depositional environments. Alluvial basin stratigraphy is of significant importance when reconstructing paleoclimate of landscapes as they contain the most complete record for quantitative analysis of Earth's terrestrial surface deep into geologic time (e.g. Sloss, 1962; Ager, 1973; Paola, 2000). Understanding and modeling alluvial basin evolution is of further importance because fluvial strata can form high net-to-gross producing hydrocarbon reservoirs (Tyler and Finley, 1991; Bowman et al., 1993; Salter, 1993; Laure and Hodavik, 2006; Labourdette, 2011) and significant aquifers (Guin et al., 2010; Ronayne et al., 2010). In addition, as we look to the future, fluvial strata may play an important role in the removal of atmospheric carbon because depleted hydrocarbon reservoirs are likely candidates for carbon sequestration (Holloway, 2001; Bruant et al., 2002; Pruess and Garcıa, 2002; Bachu, 2003; Kovscek and Cakici, 2005; Kovscek and Wang, 2005; Deng et al., 2012; Dai et al., 2014). However, quantitative modeling and prediction of alluvial stratigraphic patterns are particularly difficult due to the large spatial and long timescales surface conditions and processes operate on. The geologic community is currently capable of creating complex and noisy deterministic models of deposition that produce realistic stratigraphy, but experimental data sets suggest the numerical models are too "active" (too frequent events of erosion/deposition) and may underrepresent periods of geomorphic stasis (Straub and Foreman, 2018). In fact, in some ways the sedimentary community may be overcomplicating depositional models (Straub et al., 2020). For example, it appears major changes in the spatial distribution of depositional environments in a basin can be largely explained and captured with mass balance approaches to sediment volumes, whereas previous approaches invoked fundamental changes in fluvial and fluviodeltaic dynamics (Paola and Martin, 2012;

Hampson et al., 2014). As we continue to improve our capacity to reconstruct paleoenvironmental conditions from stratigraphy and perform stratigraphic prediction, it is wise to expend our efforts on better understanding the primary, first-order processes vital to constructing stratigraphy rather than focusing exclusively on building increasingly complex models.

Stratigraphy is created through sedimentary patterns developed by changes in allogenic conditions (e.g., climate, tectonics, sea level) and through autogenic processes (e.g., storage and release, channel avulsion, lobe switching). Distinguishing autogenic variations from allogenic signatures is key to understanding paleoenvironmental influences on the rock record. Non-steady external forcings such as the rate of eustatic base-level change or tectonic sediment flux are traditionally viewed as of primary importance in the development and characteristics of stratigraphy due to their large magnitude fluctuations and operation over long time scales. Traditionally in the literature autogenic processes have been thought of as background "noise" generators and are not understood sufficiently to identify autogenic signatures uniquely (Kim and Jerolmack, 2008). The characterization of autogenic processes as stochastic noise has become a sort of null hypothesis or condition for stratigraphic variability. Interestingly though, recent studies have shown that fluvio-deltaic autogenic geomorphic behaviors can be cyclic in nature, however their stratigraphic signatures (e.g. bed thicknesses, periods of stasis, or length and frequency of erosion) have not been clearly defined (Mohrig et al., 2000; Paola, 2000; Heller et al., 2001; Muto and Steel, 2001; Paola et al., 2001; Sheets et al., 2002; Ashworth et al., 2004; Muto and Steel, 2004; Hickson et al., 2005; Jerolmack and Mohrig, 2005; Kim et al., 2006; Kim and Muto, 2007; Kim and Paola, 2007; Kim and Jerolmack, 2008; Paola et al., 2009). Although these autogenic behaviors have been described as “cyclic”, the sedimentary community does not have a clear,

unified, and agreed upon definition for what we mean when we say “cyclic.” Does “cyclic” require regularity in the time domain or simply repetitions?

Autogenic processes likely operate on temporal scales similar to several allogenic forcings, making it potentially difficult to disentangle whether autogenics or allogenics is responsible for a given depositional pattern. One such group of allogenic forcings is the Milankovitch orbital cycles. The Milankovitch cycles represent variations in the Earth’s orbital movement; namely, the shape of Earth’s orbit (eccentricity), the angle of Earth’s tilt axis (obliquity), and the direction of Earth’s axis rotation (precession). These variations in Earth’s orbital movement change the amount and spatial distribution of insolation that reaches the atmosphere, thus affecting long-term climate. The cycles in climate occur on the timescales of $10^4$ to $10^5$ years, overlapping with basin-filling timescales of sediment supply.

In lacustrine environments, evidence for climatically-linked and orbitally-forced sedimentary cycles has been established in such areas as the Triassic Newark Basin of the eastern United States, Eocene Green River Formation of Western Interior of the United States, and Mediterranean Neogene strata amongst other areas (Olsen et al., 1996; Abdul Aziz et al., 2003; Machlus et al., 2008). Yet, lacustrine sedimentation is considered more uniform, complete, and major unconformities more readily identifiable lithologically. In the absence of significant drops in lake level, widespread reworking of sediments, a part from bioturbation, is rare. In contrast, the stratigraphic products of fluvio-deltaic systems are considered to be less sensitive to astronomically-forced climate change than lacustrine systems (likely due shorter advection length-scales; Ganti et al., 2014). Fluvio-deltaic systems are also susceptible to signal shredding and incomplete preservation via storage and release events.

Recently though, Westerhold et al. (2007) identified precession and eccentricity driven climate cycles in deep sea Paleocene-Eocene stratigraphy, and others (Abdul Aziz et al., 2008; Abels et al., 2013; Westerhold et al., 2018) found contemporaneous precession driven autocyclic stratigraphy in the upper Paleocene-lower Eocene Willwood Formation of the Bighorn Basin, Wyoming that are purely alluvial in genesis. These proposed orbitally-forced cycles are represented by variation in floodplain paleosol development, which is feasibly sensitive to both paleoclimate and floodplain topography driven by channel morphodynamics (Kraus and Gwinn, 1997). In order to truly decouple autogenic cyclicity from allogenic signatures in fluvial systems, the sedimentary community must investigate autogenic responses during both steady and non-steady external conditions. Ideally, the periodicity of autogenic processes would be constrained. Are they cyclic with a known, regular frequency? Or are they simply repetitive without cyclicity?

One important autogenic process recognized in the alluvial stratigraphic literature is termed the compensation time scale. The compensation time scale ($T_{comp}$) measures the time necessary for a fluvio-deltaic system's channel to move and deposit across a basin and for subsidence to remove those deposits from the superficial zone of reworking (Sheets et al., 2002; Wang et al., 2011; Straub and Wang, 2013; Straub and Esposito, 2013). Another way of conceptualizing this is that the compensation timescale is the timescale on which accommodation, created by subsidence, dictates the movement and position of the sediment routing system. Filling of accommodation space is the central tendency of sediment routing systems and the compensation timescale describes the time over which the fluvio-deltaic system is filling that accommodation efficiently. It is not yet known if this autogenic behavior is cyclical or merely repetitive.

The compensation timescale is a consequence of the long-term sedimentation rate and channel avulsion in alluvial systems. The long-term sedimentation rate is a proxy for the long-term

subsidence rate of the basin (Xie and Heller, 2009). In tectonic basins, this long-term subsidence is linked to the mechanical properties of the lithosphere and mimics the flexural rate of the lithosphere (Walcott, 1970). This rate of flexure is a near constant that changes slowly and smoothly over meso- to long-timescales (Walcott, 1970). In some types of basins this will not be the case, for example some rift or oblique-slip basins where normal faulting creates accommodation (Xie and Heller, 2009). The combination of the stable long-term sedimentation rate and cyclic channel avulsion creates determinisitic depositional patterns that could exhibit some periodicity.

Although field studies of the compensation time scale are still in their early stages it appears to occur on a similar temporal scale as Milankovitch-scale climate variations or longer (Foreman and Straub, 2017; Trampush et al., 2017). If the compensation time scale occurs periodically, it is possible that some previously identified allogenic forced cyclic stratigraphy could be misidentified as autogenic compensation time scale cycles. Therefore, it is important to investigate and identify compensation time scale cyclicity to rule out misidentified cycles.

In my study, I statistically analyzed experimentally produced stratigraphy under steady external forces to determine if the cyclicity of autogenic behaviors (specifically the compensation time scale) may be preserved stratigraphically in the absence of external forcings. These results are compared to similarly analyzed data from the upper Paleocene-lower Eocene Willwood Formation of the Bighorn Basin to determine if cycles in bed thicknesses are present and whether they match up to the estimated compensation timescale, precession, or other known cyclic processes. The Willwood Formation is a purely alluvial depositional system that is ideal for my study because there are multiple, time equivalent, nearly complete cores that allow for precise bed thickness measurements.

## 2. Background

### *2.1. Stratigraphic Experiments & Compensation Time Scale*

Laboratory-scale, “sand box” experiments allow for the independent control of base level, water discharge, sediment input, and other parameters while allowing the sedimentary system to freely develop according to its own internal physics (Paola et al., 2009). Much of stratigraphic experiments' effectiveness is not in their ability to recreate specific real-world systems, but to examine scale-independent variables compared to modern basins (Paola et al., 2009). Laboratory-scale experiments are an optimal resource for testing numerical and conceptual stratigraphic models because the boundary conditions are controlled and known, the depositional system is simpler, and temporal scales are shorter than for natural basins (Kim and Jerolmack, 2008; Paola et al., 2009; Straub et al., 2009; Straub and Wang, 2013). These attributes allow researchers to observe and quantify the topographic evolution of a system and processes such as avulsion in rivers, storage and release patterns, and lobe switching on deltas that dictate said stratigraphic evolution. Laboratory scale experiments are uniquely ideal for testing the hypothesis of interest herein because the long-term sedimentation rates remain constant, the precise start and end times of the experiment are known, and the external forcings are removed to create a purely autogenic basin.

Subsidence creates accommodation space and accommodation space is filled via sediment transport systems. The compensation time scale as a concept has its origins within experimental stratigraphic studies and represents an autogenic behavior that measures the time necessary for large-scale transport systems to smoothly distribute sediment across the basin (Sheets et al., 2002; Wang et al., 2011; Straub and Esposito, 2013; Straub and Wang, 2013). Compensation is the

tendency for a sediment transport system to occupy topographic lows. This time scale is an intrinsic feature of the depositional system and produces autogenic patterns that actively fill stratigraphic gaps. The compensation timescale marks the shift from deposits placed randomly to deterministically stacking. $T_{comp}$ is a result of the combination of geomorphic topographic variability and subsidence. This combination creates uneven accommodation space that is filled by compensational deposition. While autogenic behaviors operate at a variety of temporal scales, the compensation time scale can be reasonably well constrained by dividing the topographic roughness (an estimate of the maximum flow depth in basins dominated by non-cohesive sediment supply) by the long-term sedimentation rate (Wang et al., 2011). This is likely a simplification and there are several nuances to the compensation timescale yet to be resolved, but to a first approximation it does appear it can be recovered in both experimental and field systems (Trampush et al., 2017). In field systems, the minimum estimate of the topographic roughness can be estimated as the maximum flow depth. However, Trampush et al. (2017) suggests that the most likely estimation is the median sandbody thickness which represents a zone of channel migration and local avulsion that can create topographic highs and lows.

In experimental systems the compensation time scale is thought to act as a low-pass filter for fluctuations in relative sea level when the fluctuations occur on shorter time scales than $T_{comp}$ in fluvio-deltaic experiments (Li et al., 2016). The compensation timescale is also an effective low-pass filter when the relative sea level changes have amplitudes smaller than the topographic roughness of the system. Thus, in experimental systems in order for an allogenic behavior to be recognized and differentiated from background stochastic depositional events, the allogenic forcing must be of either longer duration and/or greater amplitude than the compensation time scale (Li et al., 2016). The compensation timescale has also been identified as a filter for

geochemical climate signal proxies requiring climate cycles to be twice the compensation time scale in order to prevent shredding and signal loss, signal aliasing, and/or spurious climate cycles (Foreman and Straub, 2017; Trampush and Hajek, 2017). However, in my study I focus exclusively on the strata potentially produced by autogenic processes and allogenic forcings rather than proxy records contained within the stratigraphy.

### *2.2. Geologic Setting of the Bighorn Basin*

The Bighorn Basin of northwest Wyoming, U.S.A., contains a well studied, extensive history of early Paleogene alluvial deposition. The basin formed during the Laramide Orogeny, which involved the segmentation of the former Sevier foreland basin system into a series of intermontane basins separated by basement-involved uplifts during the Late Cretaceous through Paleogene (Dickinson et al., 1988; Lawton, 2008). The Bighorn Basin is surrounded on three sides by the Pryor Mountains to the northeast, Bighorn Mountains to the east, the Owl Creek Mountains to the south, the Absaroka Mountains to the southwest and west, and the Beartooth Mountains to the northwest (Fig. 2a). These uplifts provided both the detritus and the subsidence from lithospheric flexure that preserved over two kilometers of alluvial sedimentary strata (Bown, 1980; Clyde et al., 2007; Secord et al., 2008). Six nearly complete cores were drilled at three localities in the Willwood Formation in 2011 as part of the Bighorn Basin Coring Project funded by the National Science Foundation. The majority of these cores have well-constrained ages which allows for precise sedimentation rate estimations (Clyde et al., 2007). As such, the latest Paleocene and early Eocene sediments of the Willwood Formation are of particular relevance to my study (Bown and Kraus, 1981; Clyde et al., 2007; Secord et al., 2008).

The Willwood Formation is dominated by alluvial deposition and characterized by the presence of extensive red beds representing well-drained floodplain soils (Kraus and Middleton, 1987; Kraus and Gwinn, 1997; Kraus, 2001; Kraus and Riggins, 2007). There are three important lithofacies associations in the Willwood Formation (Fig. 3). The first lithofacies association contains red, yellow, orange, and purple mottled siltstone and claystones (Fig. 3b,c,d). The colors associated with these mudstones correlates to the type and amount of iron oxide present in the samples with hematite responsible for redness and goethite responsible for yellow colorations. The purple areas have an intermediate iron oxide content. The mix of hematite and geothite indicates that the mudstones are pedogenically-modified soils on the floodplain, redder paleosols are indicative of better drained and drier conditions relative to purple paleosols (Kraus, 2001). The second lithofacies association is composed of heterolithic, "avulsion" sequences containing abundant, thin tabular sandstone units and lenticular sandbodies (Fig. 3c,d). Most of the sandstones in the heterolithic sequences are classified as ribbons with a width/thickness ratio less than 10. They have a scoop shaped bottom that cuts into as much as 5 m of the underlying paleosols. These sequences record crevasse splays and minor floodplain channel deposition associated with the initiation of avulsion (Kraus, 2001). The third lithofacies association are multi-story sheet sandbodies with a width/thickness ratio over 100 (Fig. 3a,b,c,d). The base of these sandbodies contain mudstone intraclasts and carbonate nodules from the erosion of age equivalent soils. These sandbodies represent major fluvial conduits for sediment in the basin that contain bar clinoforms, channel scour surfaces, and both dune and ripple cross-stratification (Kraus and Middleton, 1987; Kraus and Gwinn, 1997; Kraus, 2001).

The Willwood Formation contains the most extensive and refined terrestrial record of early Paleogene paleoclimate and paleobiology in the world (Koch et al., 1992; Clyde and Gingerich,

1998; Gingerich, 2001; Wing et al., 2005; Smith et al., 2007; Abdul Aziz et al., 2008; Abels et al., 2012; Snell et al., 2013). Several studies have identified perturbations and fluctuations in the contemporary warm, greenhouse conditions that affected environments in the basin. Most thoroughly documented is the Paleocene-Eocene Thermal Maximum (PETM) that occurred ~56 Ma, which caused global temperatures to rise 5-8°C for approximately 200 kyrs (Zachos et al., 2001; Murphy et al., 2010; McInerney and Wing, 2011; Westerhold et al., 2018). This event is associated with ca. 5°C of warming in the Bighorn Basin, and is linked to a massive release of isotopically-light, exogenic carbon into Earth's oceans and atmosphere, likely from methane clathrates (Bowen et al., 2001; Zachos et al., 2001; Wing et al., 2005; Zachos et al., 2010; Snell et al., 2013). The event is identifiable in marine and terrestrial stratigraphy by an abrupt negative carbon isotope excursion in a variety of geochemical proxies (McInerney and Wing, 2011).

In the Bighorn Basin, the PETM event is associated with the arrival of perissodactyls, artiodactyls, primate mammal orders, vegetation overturn, and a drying of and/or increase in the seasonality of precipitation (Clyde and Gingerich, 1998; Wing et al., 2005; Kraus and Riggins, 2007; Kraus et al., 2015). The vegetation and hydrologic changes likely caused shifts in soil development and river dynamics during the PETM (Kraus and Riggins, 2007; Foreman, 2014; Kraus et al., 2015; Baczynski et al., 2019). Furthermore, the basin records several additional hyperthermal events that post-date the PETM—these are smaller in magnitude and shorter in duration, which potentially occur with Milankovitch periodicities (Zachos et al., 2010). The most notable paired Eocene Thermal Maximum (ETM) 2 and the subsequent H2 hyperthermal events ~ 53 Ma were both approximately 50 kyrs in duration (Abels et al., 2012; 2016). Finally, remarkable precession-scale variability (i.e., ~ 20 kyrs) in soil development has been proposed both within the PETM and during background climate states between hyperthermals (Abdul Aziz et al., 2008;

Abels et al., 2013; 2016). It is hypothesized that orbitally-driven shifts in rainfall and river discharge induced alternating phases of floodplain deposition between an overbank depositional phases with a constrained river channel and extensive paleosol development to an avulsion phase characterized by a comparatively unconstrained river channel and abundant crevasse splays as the channel searches for a new location to establish itself (Abels et al., 2013).

## 3. Materials and Methods

### *3.1. Stratigraphic Experiment*

Experimental datasets used in my study are from experiment TDB-10-1 performed by Straub and Wang (2013) at Tulane University's Sediment Dynamics Laboratory. This experiment was created as a control in a study of the compensational behavior of a fluvio-deltaic system under constant boundary conditions (Straub and Wang, 2013). The experimental basin was 2.8 m wide, 4.2 m long, and 0.65 m deep (Fig. 1b), and input conditions held the water discharge of 0.451 liters/s and sediment discharge of 0.011 liters/s constant throughout the experiment (Straub and Wang, 2013). Accommodation was created through constant, spatially-even base-level rise at 5mm/hr using a computer-controlled weir. This combination of boundary conditions created a purely aggradational fluvio-deltaic system (Straub and Wang, 2013). While this experiment was not designed for my study, it is ideal for this analysis because its constant boundary conditions and simple design create a system that relies purely on autogenic processes to create stratigraphy.

The sediment fed to the experimental basin was a mixture of 70% quartz sand and 30% coal sand, which roughly represent the coarse and fine components of a natural system, respectively. Despite their different grain sizes ($D_{50}$= 110 mm for quartz and $D_{50}$ of 440 mm for

anthracite), the difference in transport behavior is driven primarily by their respectively different specific gravities of 2.65 and 1.3. Overall, this experimental setup, methodology, and approach is a variant of many previous deltaic experiments evaluating scale-independent phenomena in sedimentary basins (e.g. Sheets et al., 2002; Paola et al., 2009; Wang et al., 2011; Straub and Esposito, 2013; Straub and Wang, 2013). In total, the TDB-10-1 experiment ran for 78.2 hours after its initial build-out phase.

In addition to overhead photographs, Straub and Wang (2013) took high-resolution topographic laser scans in the basin every two minutes along three strike-oriented transects (proximal, medial, and distal to the sediment source; Straub and Wang, 2013). My study focuses on data, obtained via SEAD Internal Repository, from the proximal transect wherein the stratigraphic sections at one hundred randomly selected localities are analyzed (Fig. 1c). The proximal transect is ideal for my study because it most closely aligns with the alluvial depositional environment of the field data rather than more distal portions of the experimental delta near sea level. These topographic data allow the precise tracking of erosion, deposition, and stasis—as well as the production of a synthetic stratigraphic record of beds deposited in a basin exclusively influenced by autogenic processes (Fig. 1a). Straub and Wang (2013) found that the topographic roughness of the experimental surface scaled with the maximum flow depth of channels on the experimental surface (18.5 ± 0.5 mm). This maximum flow depth was used to calculate a $T_{comp}$ of 222 min for the fluvially-dominated portion of the sedimentary system.

The first step in the data analysis is to assign the preserved beds an age based on linear interpolation between the start and end experimental runtime and total thickness of accumulated sediment. The assumption of linear sedimentation rates is commonly made when constructing age models of sedimentary strata (e.g. Wilf et al., 2003; Sommerfield, 2006; Clyde et al., 2007; Trauth,

2014). Herein, I have the advantage that I know *a priori* that on experimental basin-filling time scales that long-term sedimentation and subsidence rates are constant (Straub and Wang, 2013). Each bed, following this constancy, had a specific thickness and time of deposition. Subsequently, a time series analysis is performed using the software Past version 3.16 (Hammer et al., 2001). I used the REDFIT protocol with n = 1000 Monte Carlo simulations of the autoregressive (AR1) process, oversampling and segmentation were set to 1, and a Blackman-Harris window. This protocol seeks to account for stochastic variability in climate records that is characterized by red noise as opposed to white noise. Red noise displays a decrease in spectral amplitude with increasing frequency of variation, white noise has no such relationship. The AR(1) or autoregressive process captures the partial dependence of the current state or condition with the previous state or condition of the system. In paleoclimate studies, this can be interpreted as the climate at time interval "*t*", is at least partially dependent upon the climate state at some point in the past, time interval "*t-1*". The 1000 Monte Carlo simulations of this process creates a comprehensive set of purely stochastic variation from which any regular, peridoic signal in the observed data can be judged against. The Monte Carlo simulation encompasses the probablility "space" of outcomes generated by stochastic red noise. It describes the world of random cycles that correspond to red noise. If the observed data falls out side this range, it is likely a "real" climate signature or cycle. A spectral analysis also requires the choice of a window function, which partially determines the zone over which the fourier transform operates to decompose the time series function into a function that describe the temporal frequency of the pattern. There are multiple choices (e.g., rectangular, triangular, Welch), but the Blackman-Harris is common in paleoclimate studies and is form of cosine window. The 99% confidence limit is used to identify statistically meaningful cycle frequencies. This is a standard methodology for time series analysis

of unevenly sampled signals, and has been previously used for paleoclimate records (Hammer et al., 2001; Schulz and Mudelsee, 2002; Foreman and Straub, 2017). Each of the hundred randomly selected localities is subjected to the same analysis.

### *3.2. Bighorn Basin Core*

Field datasets used in my study are from the Bighorn Basin Coring Project (BBCP), which drilled three localities within the basin in 2011 (Fig. 2a). Six cores were obtained (two at each locality) with over 98% core recovery of 900 total meters of early Paleogene alluvial stratigraphy (Clyde et al., 2013). The cores were drilled, processed, and described according to IODP coring protocol by the BBCP science team (Clyde et al., 2013). Summaries of the coring procedures and methodologies are outlined elsewhere (Clyde et al., 2013). Interestingly these cores have already produced new, ultra-high resolution paleoclimate records in the basin (Bowen et al., 2015; Maxbauer et al., 2016; D'Ambrosia et al., 2017; Westerhold et al., 2018). My study uses cores recovered at Polecat Bench (PCB-2A, PCB-2B) and Gilmore Hill (GMH-3A), as described by the BBCP science team party in 2012, to constitute the data for detailed records of bed thickness (Fig. 2b). These bed thicknesses were measured by the BBCP science team using visual description of halved cores (Clyde et al., 2013). Visual description is a common core practice where scientists use identifying properties (e.g. grain size change, sedimentary structures, bedding surfaces) to define beds. Core data offer the opportunity to describe bed variation in greater detail and resolution than outcrop data wherein modern, surficial weathering can obscure bed contacts.

In an effort to ensure data integrity, cores from the Basin Substation location and core GMH-3B are not used due to larger uncertainties in long-term accumulation rates at the Basin Substation location and shorter stratigraphic thickness recovered from core GMH-3B at Gilmore

Hill. Additionally, these aspects of the cores were key factors that inhibited confidence and application of the time series analyses. The PCB-2A, PCB-2B, and GMH-3A cores analyzed herein are 130.0 m, 245.1 m, and 202.4 m long, respectively. The PCB core spans the PETM hyperthermal event (Bowen et al., 2015).

The majority of the GMH core predates the ETM2/H2 hyperthermal event and captures background early Eocene climate state in the Bighorn Basin. Contrastingly, though, the uppermost sandstone units preserved in the core may correlate with the hyperthermal (Abels et al., 2012; Clyde et al., 2013). This sandstone unit is not included in the analysis, as my analysis is restricted to overbank facies to mirror Abels et al. (2013) data collection. A combination of magnetostratigraphy, biostratigraphy, isotope stratigraphy, and sparse radiometric dates constrain the accumulation rates for these two locations. The best estimates for the long-term accumulation rate at Polecat Bench is 390 m/Myrs and at Gilmore Hill it is 329 m/Myrs (Clyde et al., 2007; Abdul Aziz et al., 2008; Abels et al., 2013). Based on these long-term accumulation rates, each individual bed identified in the cores is assigned a linearly-interpolated age and is submitted to the same time series analysis as the experimental datasets to assess potential cyclicity in bed thicknesses. The cores drilled at Basin Substation are not used for this analyses because the age constraints are not well defined.

I estimated the topographic roughness using median channel flow depths, maximum channel flow depths, median sandbody thicknesses, and maximum sandbody thicknesses (data from Kraus and Middleton, 1987; Foreman, 2014; Owen et al., 2017). This provides the basis for the minimal compensation timescale and likely longest compensation timescale. Channel flow depth is calculated using the median and maximum bar clinoform vertical relief. Mohrig et al. (2000) presents data that indicate paleo-river flow depths can be captured by the thickness of bar

clinoforms. River bars, whether point bars or braid bars, represent common “macro-forms” that fill channels. Their thickness is restricted by the depth of bankfull flow. Sandbody thicknesses are estimated using recognizable scour surfaces and fining up sequences in both grainsize and sedimentary structures that capture the bedforms typically encountered within a river channel (i.e. conglomerates at base, large scale dunes, small scale dunes, and ripples; Kraus and Middleton, 1987). Instead of using the median flow depth as the most likely topographic roughness estimate, I use the maximum channel flow depth and sandbody thickness because it is more appropriate for field scale systems rather than experimental systems. This is likely due to cohesive properties of real world alluvial systems (Trampush et al., 2017).

### *3.3. Bed Thickness Distribution*

Bed thicknesses were plotted to determine if they distribute normally, log-normally, exponentially, or by power law. The approach used here is similar to previous turbidite studies where the output statistic (bed thickness (*h*)) is compared to the assumed or known input statistic (this being sediment volume at the time of deposition (*N*)) (Malinverno, 1997; Carlson and Grotzinger, 2001; Mattern, 2002; Sinclair and Cowie, 2003; Clark and Steel, 2006). The sediment volume at the time of deposition can be understood as the number of beds thicker than *h*. Five randomly selected samples from the experimental dataset are, then, compiled into one plot. Each of the cores, PCB-2A, PCB-2B, and GMH-3A are examined separately. Bed thicknesses from both the experimental and field datasets are binned based on the range of thicknesses present in the sample. Distribution type is determined by regression trendline reliability based on the highest $R^2$ value.

## 4. Results

### *4.1. Stratigraphic Experiment*

Topographic data and the resultant synthetic stratigraphic sections from TDB-10-1 were used to test the hypothesis that an alluvial system subject to static boundary conditions will produce an autogenic stratigraphic record that contains cycles of deposition with regular periodicities. Indeed, spectral analyses of the experimental bed thicknesses revealed statistically significant cycles (at the 99% confidence interval) in 67% of the tested vertical sections (Fig. 4a,b) with 93 total cycles observed (Table 1). Identified peaks within the power spectra, though, do not display the same cycle period (Fig. 4). The mean and median frequencies are 2.426 and 2.491 times that of the compensation timescale, respectively, but the range of identified frequencies is 0.2777 to 5.162 times the compensation timescale. The primary motivation of the study was to determine if the compensational timescale created cyclic bed thicknesses. Statistically significant cycles occurred at periods both longer and shorter than the compensation time scale in 63% of the sections analyzed (Fig. 4a,b). Cycle periods that closely approximated $T_{comp}$, based on the error bounds of the compensation timescale calculated using the ± 0.5mm laser precision, were found in only 4% of the sampled sections (Fig. 4c). Statistically significant frequencies tended to occur at shorter periods than the compensation time scale (Fig. 5).

### *4.2. Bighorn Basin*

The PCB-2A, PCB-2B, and GMH-3A cores were analyzed using the same time series analysis as the experimental data. Spectral analysis of PCB-2A, PCB-2B, and GMH-3A revealed

statistically significant peaks at 3.5 kyrs, 3.7 kyrs, and 15.0 kyrs (respectively) at the 99% confidence limit (Fig. 6a,b). At the two localities, Polecat Bench and Gilmore Hill, the values of $T_{comp}$ were derived using different estimates of topographic roughness divided by the long-term accumulation rate for that location in the basin.

At Polecat Bench topographic roughness was estimated from median river flow depths (1.2 m), maximum river flow depths (4.3 m), median sandbody thickness (8.7 m), and maximum fluvial sandbody thickness (33 m) to produce $T_{comp}$ of 3.0 kyrs, 11.0 kyrs, 22.3 kyrs, and 84.6 kyrs for this area in the basin. A compensation timescale of 3.0 kyrs is near the range of the 3.5 and 3.7 kyrs cycles in floodplain strata identified in the Polecat Bench cores. However, that compensation timescale is calculated using the median river flow depths which is likely a significant underestimate of topographic roughness (see Discussion below). Similarly, at the Gilmore Hill, topographic roughness was estimated from median river flow depths (1.8 m), maximum river flow depths (4.1 m), median sandbody thickness (8.0 m), and maximum fluvial sandbody thickness (21.7 m) to produce $T_{comp}$ of 5.5 kyrs, 12.5 kyrs, 24.3 kyrs, and 66.0 kyrs. Again, none of these corresponded to the identified bed cycle frequency (Fig. 6b). It should be noted that 12.5 kyrs is near the 15 kyrs compensation timescale, but is not within the uncertainty bounds to consider it a match.

### *4.3. Bed Thickness Distribution*

The bed thickness distributions of PCB-2A, PCB-2B, GMH-3A and a selection of five sections of TDB-10-1 were graphed on a log-log probability of exceedance plot (Fig. 7). Each of the distributions have an exponential trendline with high $R^2$ values (Fig. 7), which provided the best fit as compared to linear, logarithmic, and power law (Table 2). Equations and $R^2$ values for

each trendline can be found in Table 2. Despite, PCB-2B recovering 115 meters more of core compared to PCB-2A, the best fit equations are similar (Table 2). Thus, the bed thickness distribution is similar despite PCB-2B being longer and containing more data. Bed thicknesses show notable deviation from the trend lines at approximately the same place in each of the plots. The PCB and GMH-3A cores exhibit the deviation between beds thicker than 1.4m and 1.6m. These deviations occur within the range of the median flow depths of the channels. This differentiation could mark the difference between channelized beds and overbank deposits and crevasse splays.

## 5. Discussion

### *5.1. Statistical Distribution of Bed Thicknesses*

Historically, stratigraphic studies have heavily skewed towards qualitative interpretations of outcrops and core. Bed thicknesses and their incorporation into lithofacies associations are one of the most fundamental quantitative data sets collected by sedimentologists and stratigraphers. Individual beds are readily observable, usually have distinct upper and lower contacts, and require minimal genetic interpretations to measure directly. Beds are the building blocks of stratigraphy. Moreover, studies have linked their thickness patterns to the morphodynamics of the sediment transport system (Paola and Borgman, 1991). For example, the relative rates of translation and aggradation of dunes and ripples controls the geometry of cross-bed sets (Best, 2005). On the scale of river channels, dune heights and their cross-bedded deposits scale with flow depth (Paola and Borgman, 1991; Myrow et al., 2018). Indeed, these relationships may be sensitive enough to identify backwater conditions in paleo-rivers (Wu et al., 2020). In marine systems the constraints

of fair-weather and storm-weather wave base have well-established, qualitative links with bed sedimentary structures (Nichols, 2009). And the quantitative characteristics of oscillation ripples have been used to estimate paleo-windspeed in the Neo-Proterozoic (Allen and Hoffman, 2005). The broader statistical characteristics of beds from different environments is not currently available in the literature.

There has been a recent focus on quantitative approaches to understanding stratigraphic processes and bed thickness distributions, but much has focused on marine systems. For example, recent studies on submarine fan stratigraphy and turbidite bed thicknesses revealed a scaling relationship:

$$N(h) = ah^{-B}$$

where $N$ is the number of layers with thickness greater than $h$, $B$ is the scaling exponent and $a$ is a constant (Rothman and Grotzinger, 1995; Malinverno, 1997). Previous researchers hypothesized that changes in the value of $B$ likely relate to depositional variations linked to the properties of the sediment transport system (Rothman et al., 1994; Rothman and Grotzinger, 1995; Carlson and Grotzinger, 2001). Log-normal, power-law, exponential, and truncated normal have all been proposed for frequency distributions of bed thicknesses in sediment gravity flows, predominantly turbidites. Power law distributions appear to be the most common, though interestingly, departure from power-law distribution may be linked to the sub-environment on the submarine fan. Deviation from power-law distribution or log-normal distribution, more specifically, suggests increased channelization and bed amalgamation, thus implying fan-lobe deposits (Carlson and

Grotzinger, 2001). It has been suggested that similar scaling relations can be linked to other dynamic systems (Kardar et al., 1986; Carlson and Grotzinger, 2001).

The statistical distributions observed in my study follow an exponential trend that diverges from the log-normal and power law distributions seen in previous studies on submarine fan deposits (Carlson and Grotzinger, 2001), yet the exponential distribution matches previous analyses of alluvial bed thicknesses. Data sets that document large (100+) bed thickness measurements in alluvial strata are rare, likely due to data collection being highly labor-intensive. Experimental alluvial system allow the rapid collection of this type of data that yield insights. Indeed experiments allow near instantaneous erosion, deposition, and bed thickneses to be measured independently. From these data exponential bed thickness distributions are hypothesized to be created in basins with near symmetric magnitidue-frequency distributions of erosion and deposition augmented with surfacial reworking- cut-and-fill stratigraphy (Straub et al., 2012). Cut-and-fill here refers to the behavior of a transport to create topographic lows via erosion and preferentially fill them with thicker deposits. The experimental and field examples used in my study contain incontrovertible evidence of fluvial channel reworking the surface (Wing et al., 2005; Wang et al., 2011; Foreman, 2014). Mapping of topography in experiments can be linked explicitly to channel occupation events. And in the Willwood Formation case study, scour surface and cut-and-fill structures have been directly observed with fluvial sandbodies intersecting subjacent floodplain strata (Wing et al., 2005; Foreman, 2014). This cut-and-fill deposition provides a likely explanation for the deviation observed in the bed thickness distribution plots.

The deviations on the bed thickness distribution plots in both the experimental and field studies correlate to the median channel depths of the systems. In a cut-and-fill depositional system, the channel reworks the surface and cuts into existing sediment. The channel acts as a filter on bed

thicknesses and limits the majority of bed thicknesses to be at or less than the channel depth. In the case of alluvial systems, the beds thicker than the median channel depth correlate to sudden depositional events such as crevasse splays or from long-term accumulation similar to the well-developed paleosols in our field data set. Interestingly, the deviation observed in our study is present but not addressed in other bed thickness distribution charts from a wide variety of depositional environments (alluvial/fluvial, submarine fan, lacustrine, and aeolian) on both on Earth and Mars (e.g. Malinverno, 1997; Carlson and Grotzinger, 2001; Talling, 2001; Stack et al., 2013). Since the deviation is not addressed, it is difficult to determine at which thickness this phenomena occurs in other studies. The deviation could be tied to a similar depositional control on bed thicknesses in other systems. For example, if the hypothesis holds, proximal submarine fan bed thickness distributions are likely to exhibit the deviation at median flow depth of the submarine channel, similar to what is seen in proximal alluvial systems. In a distal submarine fan or lacustrine environment, deposition is less event based and more a result of suspension settling. The larger beds in this environment are tied to long periods of hiatus where deposition is happening slowly; similar to soil development seen in a floodplain. These distal, suspension dominated environments may not exhibit the deviation in bed thickness distribution since there is not an geomorphic process with a focused, erosional vertical scale.

### *5.2. Stratigraphic Experiment*

The compensation time scale does not appear to be cyclic based on the experimental data. This means, that although, compensation is a repetitive process, it does not occur on a predictable and consistent timescale. Given that the compensation timescale is known, one would expect to see a robust data set of the same periodicity across several stratigraphic sections in order to deem

it cyclic. In this case, only 4% of stratigraphic sections show a statistically significant "cycle" at the compensation timescale. A sediment routing system will produce uneven stratigraphy across a basin, proximal-to-distal, and laterally. This is what is thought to create apparent cyclicity, lobes, or accumulations of sediment in some areas. While, cycles do not need to be observed at all locations at all times, a robust cycle should be present on the basin-scale and observable in a nontrivial number of stratigraphic section. Also, where observed, the cycles should display similar periodicities. A pattern that is only represented in 4% of sections does not meet the criteria of being basin-scale. It is possible that the experiment did not run long enough to capture the vertical scale necessary to preserve a cyclic signature; however, this is unlikely since the experiment ran for more than 21 times the compensation timescale. In a "field-scale" basin this could easily be comparable to over 0.5 million years of deposition. It is more likely that the compensation time scale is not cyclical. In order for the compensation time scale to be cyclic, it is assumed that basin-wide occupation of the channel and reworking occurs at the same interval over and over. Since channel avulsion is the driving mechanism that allows for sediment to be deposited across the basin, this would mean that channel avulsion would need to occur at consistent periods. It is more likely that the compensation time scale represents the maximum amount of time necessary for this behavior to occur. Therefore, compensation is happening at varying temporal scales all less than $T_{comp}$.

Autogenic "cycles", though inconsistent in spatio-temporal scale, are preserved within the experimental stratigraphy. It is difficult to assign specific processes to the signatures with the available data because there are not consistent signatures across the basin. However, it appears that there may be some localization of signatures. Such localized signatures could be a result of channel avulsion and reoccupation in the case of fluvial deposition or proximity of the river channel in the

case of overbank deposition. Given that avulsion is the driving force of compensation, and it occurs on time intervals shorter than the compensation timescale, perhaps the "cycles" present at frequencies less than $T_{comp}$ represent local channel migration.

My results may be better confirmed with basin-wide analysis instead of randomized sampling. My results could also benefit from another study running a similar experiment where autogenic processes such as channel avulsion and lobe switching are observed and timed for a comparison to the stratigraphic analysis. It is also possible that the signatures observed in the data are not translatable to autogenic processes and thus spurious. This could be further tested by looking at medial and distal locations on the delta and comparing the results to the proximal case examined here. My study focuses strictly on the proximal transect because of its correlation to the alluvial field example. However, I expect that repetitive processes like avulsion, lobe switching, and storage/release occur at different timescales down depositional dip on the delta due to channel bifurcation, change in slope, and downstream fining grain size. Similarly, experiments with cohesive sediment are another possibility for testing this hypothesis since cohesion has an effect on channel depth and avulsion frequency. If the high frequency cycles are avulsion, I expect that the mean frequency of "cycles" in a cohesive sediment would decrease because cohesion reduces channel mobility. There is, likewise, merit in examining other aspects of stratigraphy to locate autogenic cyclicity, such as duration and frequency of erosion represented by unconformities.

### *5.3. Bighorn Basin Core*

The frequencies found in the Bighorn Basin cores underestimate the compensation timescale, the sub-Milankovitch and precession cycles (7-8 kyrs and 21 kyrs) obtained in previous studies on the Bighorn Basin and Paleocene-Pleistocene marine and lacustrine successions

(Westerhold et al., 2007; Abdul Aziz et al., 2008; Abels et al., 2013). Previous Bighorn Basin studies used time series analyses of bed colors (a proxy for soil development and moisture/drainage conditions) to identify sub-Milankovitch and precession cycles (Abdul Aziz et al., 2008; Abels et al., 2013). This is different from my study because soil formation is created through weathering processes instead of depositional processes. The precession cycles have been tied to sequences of overbank and avulsion deposits where the overbank deposits represent periods of relative channel stability with some localized avulsion and the avulsion deposits represent regional avulsion caused by allogenic, astronomically-forced climate change (Abels et al., 2013). It is plausible that this avulsion was purely autogenic, thus, Milankovitch cycles were not the dominant forcing in the Bighorn Basin at the time. However, if the regional avulsion sequences were climate induced, it's possible the reason the statistical analyses do not produce the expected results is because of the influence of spurious autogenic signatures on the data. The experimental data shows autogenic processes appear to be sporadic and spatiotemporally erratic.

If the autogenic processes do not produce predictable cycles in the experimental basin, I expect that the cycles will not be preserved in the field study. The experiment is a simplified system that removes any allogenic processes from the data set—whereas, the field study is much more complex with allogenic forcings and variable sediment. Since stratigraphy is created through geomorphic processes (e.g., larger flooding events create bigger beds), climate would have to influence those geomorphic processes and that influence would have to be transferred to bed thicknesses in a predictable pattern. While this is happening, compensation is smoothing out the topographic surface and reworking the previously deposited beds. Therefore, in order to preserve a climate signal in bed thicknesses, climate would have to impart a signal with a long period or high magnitude. Recent studies indicate that the climate cycle would have to be at least twice the

compensation timescale to avoid signal shredding (Foreman and Straub, 2017). When considering the maximum flow depth estimates of the cores used to calculate the compensation timescale (best approximation based on experimental data), neither the sub-Milankovitch nor the precession cycles are long enough to prevent signal loss from compensation shredding. As such, the precession and sub-Milankovitch cycle signatures in the cores I studied have likely been shredded by compensation. Since precession cycles have a definite time estimate on Earth, compensation needs to happen quicker that what is seen in the Bighorn Basin to preserve a climate signal. The cycles present in the results are, therefore, probably autogenic signatures similar to those recorded in the experimental data. This inference suggests that basin-wide characterization of autogenic cycles cannot be made from one (or even a few) core samples—although, the number of necessary samples for confident results is unknown.

The Gilmore Hill cores represent deposits that are ~3 million years younger than the Polecat Bench and Basin Substation cores and are dominated by paleosol red beds with little preservation of less oxidized deposits. Within the Polecat Bench core there is a high incidence of paleosol red beds associated with the Paleocene-Eocene boundary. It is possible that the climatic cycles observed by Westerhold et al (2017) and Abels et al (2013) are decoupled from the bed thicknesses observed and analyzed herein. Paleosol development may be imprinted upon bed accumulation, thus the paleoclimate signature is not directly preserved by geomorphic erosion or deposition events, but rather is a secondary modifier of bed features. The paleosols found at Polecat Bench are sparse in the Basin Substation core due to reduced pedogenesis (Baczynski et al., 2019). Since these paleosols are absent, Basin Substation would be an ideal candidate for bed thickness analysis once time constraints are better defined.

Identifying and quantifying the scales and patterns of autogenic geomorphic processes (e.g., channel avulsion, lobe switching, storge and release) becomes particularly important when extracting paleoclimatic information from stratigraphy. Recent work has suggested autogenic geomorphic processes exert a fundamental control on the time resolution and completeness of climate proxy records within alluvial stratigraphy (Foreman and Straub, 2017; Trampush and Hajek, 2017). These studies highlight the role autogenic processes play on the presence of unconformities within stratigraphy creating a low pass filter on the detectable proxy-based paleoclimate signals. Yet the inherent timescales of autogenic processes and physical characteristics of the strata produced may themselves create a low pass filter on physical stratigraphy (Paola et al., 1992; Straub et al., 2020).

### *5.4 Inverse Problem*

Stratigraphic interpretation relies on correctly inverting stratigraphic patterns into driving boundary conditions. This is particularly difficult both because of the number of autogenic and allogenic processes involved in a depositional system and the number of combinations possible to create similar stratigraphic patterns. This inversion problem is at the core of this research and other ongoing stratigraphy research (e.g., Rogers, 1998; Jinnah and Roberts, 2011; Bernhardt et al., 2017). The more we learn about these depositional systems that create stratigraphic patterns, the trend appears to be moving toward the idea that “less is more” (i.e., less erosion/deposition events and more periods of stasis). For example, Paola et al. (1992) looked at the interplay of factors that cause vertical grain size changes in alluvial basins using simple 2-D diffusion models. These models generated similar stratigraphies that are largely irreconcilable without time horizons and ages of strata attributed to them.

Recent studies have started to push back on the complicated models that have been developed over time. Examples of this challenge to traditional depositional models includes recent research that shows traditional sequence stratigraphy patterns can be created via autogenic processes (Muto and Steel, 2001; Guerit et al., 2021). These studies have introduced the terms "auto-stepping" (Muto and Steel, 2001) and "auto-advance" to describe autogenic behaviors of a delta that were previously thought to only occur via allogenic forcings. In fact, stratigraphic patterns on the scale of parasequences and larger can be induced by mass balance relationships between accommodation and sediment flux as well as avulsion behaviors. As stratigraphic researchers continue to create simpler models, it is necessary that the sedimentary community fully understand the roles that autogenic and allogenic processes play in the creation of stratigraphic patterns. My study is a piece to that puzzle. To this end, I suggest the term "auto-repetitive" be adopted for stratigraphic patterns that occur with out a definitive periodicity, but future similar work should continue exploring the locations of signals created by repetitive autogenic processes such as duration and frequency of erosion and periods of stasis.

## 6. **Conclusions**

Utilizing patterns and repetition of stratigraphic products to identify cyclic patterns is not a novel concept. Whether it is using Markov chain analysis to predict repetitions in alluvial cyclothems (Gingerich, 1969) or creating elementary climate cycle curves from the stratal stacking patterns of sequence stratigraphic units (Catuneanu et al., 2011). And this approach to utilizing stratigraphic patterns to further understand the processes that created those patterns is still growing. My study attempts to further that research and unlock more information about the relationship between allogenic and autogenic patterns and the products they create.

The results of my study provide more evidence that stratigraphy modelers should recommit to the principle of parsimony. The TDB-10-1 experiment is nearly as simple of a system as one can create, long term aggradation and no allogenic changes. Yet, the stratigraphy created by the experiment is rich and complex. I am able to find bed thickness cycles at a variety of periodicities across the basin. If a modeler is given stratigraphic columns of the experimental data, their interpretation could likely invoke a far more complex depositional history than reality. This will commonly be the case in field studies where single stratigraphic sections are commonly analyzed. Furthermore, the bed thickness distribution from the simple experiment follows the same exponential trend as the more complicated field data. If simple depositional experiments create similar products to seemingly more complex, real world fluvial systems, it makes sense to limit the complexity of our stratigraphic models.

As seen above, purely autogenic systems will create repeated bed thicknesses, but these cannot be attributed to a known process. I would argue that these repeated bed thicknesses should not be referred to as cyclic. Perhaps it makes more sense to differentiate between cyclic and repetitive formally. The definition of cyclic cannot be only tied to processes that occur on predicted temporal scales. They must also occur on spatial scales beyond their immediate area. For example, Milankovitch cycles have a specific temporal scale, and their effects can be felt globally. This is dissimilar to channel avulsion which could occur recurrently, but the observed impact on stratigraphy will sometimes be restricted to smaller length-scales (i.e., in the case of local avulsion) and sometimes broader length-scales (i.e., in the case of regional avulsions). Thus, channel avulsion is auto-repetitive, not autocyclic. Otherwise, spatially nonuniform repetitions, while statistically significant, should be titled as such: repetitive. As we look forward to the future of stratigraphy, one marked by both quantitative modeling and qualitative descriptions, it is important

that we work together to build a common understanding of the language we are using to describe these repetitions or cycles.

**Data**

Experimental datasets can be obtained through the SEAD Internal Repository (http://doi.org/10.5967/M0HX19TT). Core datasets can be obtained through the International Continental Scientific Drilling Program (https://www.icdp-online.org/projects/world/north-and-central-america/bighorn-basin/).

**Works Cited**

Abdul Aziz, H., Hilgen, F.J., Krijgsman, W., and J.P. Calvo (2003). An astronomical polarity of time scale for the late middle Miocene based on cyclic continental sequences. Journal of Geophysical Research, 108(B3), 2159. https://doi.org/10.1029/2002JB001818

Abdul Aziz, H., Hilgen, F.J., van Luijk, G.M., Sluijs, A., Kraus, M.J., Pares, J.M. and P.D. Gingerich (2008). Astronomical climate control on paleosol stacking patterns in the upper Paleocene-lower Eocene Willwood Formation, Bighorn Basin, Wyoming. Geology, 36, 531–534. https://doi.org/10.1130/G24734A.1

Abels, H.A., Clyde, W.C., Gingerich, P.D., Hilgen, F.J., Fricke, H.C., Bowen, G.J. and L.J. Lourens (2012). Terrestrial carbon isotope excursions and biotic change during Paleogene hyperthermals. Nat. Geosci., 5, 326–329. https://doi.org/10.1038/ngeo1427

Abels, H.A., Kraus, M.J., and P.D. Gingerich (2013). Precession-scale cyclicity in the fluvial lower Eocene Willwood Formation of the Bighorn Basin, Wyoming (USA). Sedimentology, 60, 1467–1483. https://doi.org/10.1111/sed.12039

Abels, H.A., Lauretano, V., van Yperen, A.E., Hopman, T., Zachos, J.C., Lourens, L.J., Gingerich, P.D. and G. J. Bowen (2016). Environmental impact and magnitude of paleosol carbonate carbon isotope excursions marking five early Eocene hyperthermals in the Bighorn Basin, Wyoming. Clim. Past., 12, 1151–1163. https://doi.org/10.5194/cp-12-1151-2016

Ager, D.V. (1973). The Nature of the Stratigraphical Record. (114 pp.) Wiley.

Allen P.A. and P.F. Hoffman (2005). Extreme winds and waves in the aftermath of a Neoproterozoic glaciation. Nature, 433(7022), 123-7. https://doi.org/10.1038/nature03176

Ashworth, P.J., Best, J.L., and M. Jones (2004). Relationship between sediment supply and avulsion frequency in braided rivers. Geology, 32(1), 21-24. https://doi.org/10.1130/G19919.1

Bachu, S. (2003). Sequestration of CO2 in geological media in response to climate change: capacity of deep saline aquifers to sequester CO2 in solution. Energy Convers. Manag., 44(20), 3151–3175. https://doi.org/10.1016/S0196-8904(03)00101-8

Baczynski, A.A., McInerney, F.A., Freeman, K.H., Wing, S.L., and Bighorn Basin Coring Project (BBCP) Science Team. (2019). Carbon isotope record of trace n-alkanes in a continental PETM section recovered by the Bighorn Basin Coring Project (BBCP). Paleoceanography and Paleoclimatology, 34(5), 853-865. https://doi.org/10.1029/2019PA003579

Bernhardt, A., Schwanghart W., Hebbeln, D., Stuut, J.W., and M.R. Strecker (2017). Immediate propagation of deglacial environmental change to deep-marine turbidite systems along

the Chile convergent margin. Earth and Planetary Science Letters, 473, 190-204. https://doi.org/10.1016/j.epsl.2017.05.017

Best, J. (2005). The fluid dynamics of river dunes: A review and some future research directions. Journal of Geophysical Research, 110(F4), 21. https://doi.org/10.1029/2004JF000218

Bowen, G.J., Koch, P.L., Gingerich, P.D., Norris, R.D., Bains, S., and R. Corfield (2001). Refined isotope stratigraphy across the continental Paleocene-Eocene boundary on Polecat Bench in the northern Bighorn Basin. Univ. Mich. Pap. Paleontol., 33, 73–88.

Bowen, G.J., Maibauer, B.J., Kraus, M.J., Röhl, U., Westerhold, T., Steimke, A., Gingerich, P.D., Wing, S.L., and W.C. Clyde (2015). Two massive, rapid releases of carbon during the onset of the Palaeocene-Eocene thermal maximum. Nat. Geosci., 8, 44–47. https://doi.org/10.1038/ngeo2316

Bowman, M., McClure, N., and D. Wilkinson (1993). Wytch Farm oilfield: deterministic reservoir description of the Triassic Sherwood Sandstone. GeologicalSociety, London, Petroleum Geology Conference Series, 4(1), 1513-1517. https://doi.org/10.1144/0041513

Bown, T.M. (1980). Summary of latest Cretaceous and Cenozoic sedimentary, tectonic, and erosional events, Bighorn Basin, Wyoming. Univ. Michigan Pap. Paleontol., 24, 25–32.

Bown, T.M., and M.J. Kraus (1981). Lower Eocene alluvial paleosols (Willwood Formation, Northwest Wyoming, U.S.A.) and their significance for paleoecology, paleoclimatology, and basin analysis. Palaeogeogr, Palaeoclimatol, Palaeoecol., 34, 1–30. https://doi.org/10.1016/0031-0182(81)90056-0

Bruant Jr., R.G., Celia, M.A., Guswa, A.J., and C.A. Peters (2002). Safe storage of CO2 in deep saline aquifers. Environ. Sci. Technol., 36(11), 240A–245A. https://doi.org/10.1021/es0223325

Bryant, M., Falk, P., and C. Paola (1995). Experimental study of avulsion frequency and rate of deposition. Geology, 23(4), 365-368. https://doi.org/10.1130/0091-7613(1995)023<0365:ESOAFA>2.3.CO;2

Carlson, J. and J.P. Grotzinger (2001). Submarine fan environment inferred from turbidite thickness distributions. Journal of Sedimentary Research, 48, 1331-1351. https://doi.org/10.1046/j.1365-3091.2001.00426.x

Catuneanu, O., Galloway, W.E., Kendall, C.G.S.C., Miall, A.D., Posamentier, H.W., Strasser, A., and M.E. Tucker (2011). Sequence stratigraphy: methodology and nomenclature. Newsletters on stratigraphy, 44(3), 173-245. https://doi.org/10.1127/0078-0421/2011/0011

Cazanacli, D., C. Paola, and G. Parker (2002). Experimental steep, braided flow: Application to flooding risk on fans. Journal of Hydraulic Engineering, 128, 322- 330. https://doi.org/10.1061/(ASCE)0733-9429(2002)128:3(322)

Clyde, W.C., and P.D. Gingerich (1998). Mammalian community response to the latest Paleocene thermal maximum: an isotaphonomic study in the northern Bighorn Basin, Wyoming. Geology, 26, 1011–1014. https://doi.org/10.1130/0091-7613(1998)026<1011:MCRTTL>2.3.CO;2

Clyde, W.C., Hamzi, W., Finarelli, J.A., Wing, S.L., and A. Chew (2007). Basin-wide magnetostratigraphic framework for the Bighorn Basin, Wyoming. GSA Bull., 119, 848–859. https://doi.org/10.1130/B26104.1

Clyde, W.C., Gingerich, P.D., Wing, S.L., Röhl, U.,Westerhold, T., Bowen, G., Johnson, K., Baczynski, A.A., Diefendorf, A., McInerney, F., Schnurrenberger, D., Noren, A., Brady, K., and the BBCP Science Team (2013). Bighorn Basin Coring Project (BBCP): a continental perspective on early Paleogene hyperthermals. Sci. Dril., 16, 21–31. https://doi.org/10.5194/sd-16-21-2013

D'Ambrosia, A.R., Clyde, W.C., Fricke, H.C., Gingerich, P.D., and H.A. Abels (2017). Repetitive mammalian dwarfing during ancient greenhouse warming events. Sci. Adv., 3, e1601430. https://doi.org/10.1126/sciadv.1601430

Dai, Z., Middleton, R., Viswanathan, H., Fessenden-Rahn, J., Bauman, J., Pawar, R., and B. McPherson (2014). An integrated framework for optimizing CO2 sequestration and enhanced oil recovery. Environ. Sci. Technol. Lett., 1(1), 49–54. https://doi.org/10.1021/ez4001033

Deng, H., Stauffer, P.H., Dai, Z., Jiao, Z., and R.C. Surdam (2012). Simulation of industrial-scale CO22 storage: multi-scale heterogeneity and its impacts on storage capacity, injectivity and leakage. Int. J. Greenh. Gas Control, 10, 397–418. https://doi.org/10.1016/j.ijggc.2012.07.003

Dickinson, W.R., Klute, M.A., Hayes, M.J., Janecke, S.U., Lundin, E.R., McKittrick, M.A., and M.D. Olivares (1988), Paleogeographic and paleotectonic setting of Laramide sedimentary basins in the central Rocky Mountain region. GSA Bull., 100, 1023–1039. https://doi.org/10.1130/0016-7606(1988)100<1023:PAPSOL>2.3.CO;2

Foreman, B.Z. (2014). Climate-driven generation of a fluvial sheet sand body at the Paleocene Eocene boundary in northwest Wyoming (USA). Basin Research, 26, 225–241. http://doi.org/10.1111/bre.12027

Foreman, B.Z., and K.M. Straub (2017). Autogenic geomorphic processes determine the resolution and fidelity of terrestrial paleoclimate records. Sci. Adv., 3, e1700683. https://doi.org/10.1126/sciadv.1700683

Ganti, V., Lamb, M.P. and B. McElroy (2014). Quantitative bounds on morphodynamics and implications for reading the sedimentary record. Nat. Commun., 5, 3298. https://doi.org/10.1038/ncomms4298

Gingerich, P.D. (1969). Markov analysis of cyclic alluvial sediments. Journal of sedimentary research, 39(1), 330-332. https://doi.org/10.1306/74D71C4E-2B21-11D7-8648000102C1865D

Gingerich, P.D. (2001). Biostratigraphy of the continental Paleocene-Eocene boundary interval on Polecat Bench in the northern Bighorn Basin. Univ. Michigan Pap. Paleontol., 33, 37–67.

Guerit, L., Foreman, B. Z., Chen, C., Paola, C., and S. Castelltort (2021). Autogenic delta progradation during sea-level rise within incised valleys. Geology, 49(3), 273-277. https://doi.org/10.1130/G47976.1

Guin, A.R., Ramanathan, R.W., Ritzi, D.F., Dominic, I.A., Lunt, I.A., Scheibe, T.D., and V.L. Freedmand (2010). Simulating the heterogeneity in braided channel belt deposits: 2. Examples of results and comparison to natural deposits. Water Resource Research, 46, W04516. https://doi.org/10.1029/2009WR008112

Hammer, Ø., Harper, D.A.T., and P.D. Ryan (2001). PAST: Palaeontological statistics software package for education and data analysis. Palaeontol. Electronica 4, 9.

Hampson, G. J., Duller, R. A., Petter, A. L., Robinson, R. A. J. and P.A. Allen (2014). Mass–balance constraints on stratigraphic interpretation of linked alluvial–coastal–shelfal deposits from source to sink: Example from Cretaceous Western Interior Basin, Utah and Colorado, USA. J. Sediment. Res., 84, 935–960. https://doi.org/10.2110/jsr.2014.78

Heller, P.L., Paola, C., Hwang, I.G., John, B. and R.J. Steel (2001). Geomorphology and sequence stratigraphy due to slow and rapid base-level changes in an experimental subsiding basin (XES 96-1). American Association of Petroleum Geologists Bulletin, 85, 817-838. https://doi.org/10.1306/8626CA0F-173B-11D7-8645000102C1865D

Hickson, T.A., Sheets, B.A., Paola, C., and M. Kelberer (2005). Experimental test of tectonic controls on three-dimensional alluvial facies architecture. Journal of Sedimentary Research, 75, 710-722. https://doi.org/10.2110/jsr.2005.057

Holloway, S. (2001). Storage of fossil fuel-derived carbon dioxide beneath the surface of the earth. Annu. Rev. Environ. Resour., 26, 145–166. https://doi.org/10.1146/annurev.energy.26.1.145

Jerolmack, D.J. and D. Mohrig (2005). Frozen dynamics of migrating bedforms. Geology, 33(1), 57-60. https://doi.org/10.1130/G20897.1

Jinnah, Z.A. and E.M. Roberts (2011). Facies Associations, Paleoenvironment, and Base-Level Changes in the Upper Cretaceous Wahweap Formation, Utah, U.S.A.. Journal of Sedimentary Research, 81(4), 266–283. https://doi.org/10.2110/jsr.2011.22

Kardar, M., Parisi, G., and Y.C. Zhang (1986). Dynamic scaling of growing interfaces. Physical Review Letters, 56(9), 889. https://doi.org/10.1103/PhysRevLett.56.889

Kim, W. and D.J. Jerolmack (2008). The pulse of calm fan deltas. The Journal of Geology, 116, 315-330. https://doi.org/10.1086/588830

Kim, W. and T. Muto (2007). Autogenic response of alluvial-bedrock transition to base- level variation: Experiment and theory. Journal of Geophysical Research-Earth Surface, 112, F03S14. https://doi.org/10.1029/2006JF000561

Kim, W. and C. Paola (2007). Long-period cyclic sedimentation with constant tectonic forcing in an experimental relay ramp. Geology, 35(4), 331-334. https://doi.org/10.1130/G23194A.1

Kim, W., Paola, C., Swenson, J.B., and V.R. Voller (2006). Shoreline response to autogenic processes of sediment storage and release in the fluvial system. Journal of Geophysical Research-Earth Surface, 111, F04013. https://doi.org/10.1029/2006JF000470

Koch, P.L., Zachos, J.C., and P.D. Gingerich (1992). Correlation between isotope records in marine and continental carbon reservoirs near the Paleocene/Eocene boundary. Nature, 358, 319–322. https://doi.org/10.1038/358319a0

Kovscek, A.R. and M.D. Cakici (2005). Geologic storage of carbon dioxide and enhanced oil recovery, II, Cooptimization of storage and recovery. Energy Convers, Manag, 46, 1941–1956. https://doi.org/10.1016/j.enconman.2004.09.009

Kovscek, A.R. and Y. Wang (2005). Geologic storage of carbon dioxide and enhanced oil recovery, I, Uncertainty quantification employing a streamline based proxy for reservoir flow simulation. Energy Convers. Manag., 46, 1920–1940. https://doi.org/10.1016/j.enconman.2004.09.008

Kraus, M.J. (2001). Sedimentology and depositional setting of the Willwood Formation in the Bighorn and Clarks Fork Basin. In: Paleocene-Eocene Stratigraphy and Biotic Change in the Bighorn and Clarks Fork Basins, Wyoming (Ed. by P.D. Gingerich). Univ. Michigan Pap. Paleontol, 33, 15–28.

Kraus, M.J., and B. Gwinn (1997). Facies and facies architecture of Paleogene floodplain deposits, Willwood Formation, Bighorn Basin, Wyoming, USA. Sed. Geol., 114, 33–54. https://doi.org/10.1016/S0037-0738(97)00083-3

Kraus, M.J., and L.T. Middleton (1987). Contrasting architecture of two alluvial suites in different structural settings. In: Recent Developments in Fluvial Sedimentology (Ed. by F.G. Ethridge). Soc. Econ. Paleo. Mineral. Spec. Pub., 30, 253–262. https://doi.org/10.2110/pec.87.39.0253

Kraus, M.J., and S. Riggins (2007). Transient drying during the Paleocene-Eocene Thermal Maximum (PETM): analysis of paleosols in the Bighorn Basin, Wyoming. Palaeogeogr. Palaeoclimatol. Palaeoecol., 245, 444–461. https://doi.org/10.1016/j.palaeo.2006.09.011

Kraus, M.J., Woody, D.T., Smith, J.J., and V. Dukic (2015). Alluvial response to the Paleocene–Eocene Thermal Maximum climatic event, Polecat Bench, Wyoming (U.S.A.). Palaeogeogr. Palaeoclimatol. Palaeoecol., 435, 177–192. https://doi.org/10.1016/j.palaeo.2015.06.021

Labourdette, R. (2011). Stratigraphy and static connectivity of braided fluvial deposits of the lower Escanilla Formation, south central Pyrenees, Spain. AAPG Bulletin, 95, 585-617. https://doi.org/10.1306/08181009203

Laure, D.K., and J. Hodavik (2006). Connectivity of channelized reservoirs: A modelling approach. Petroleum Geoscience, 12, 291-308. https://doi.org/10.1144/1354-079306-699

Lawton, T.F. (2008). Laramide sedimentary basins, in Miall, A.D., ed., The Sedimentary Basins of the United States and Canada: Amsterdam, Elsevier, p. 429–450. https://doi.org/10.1016/S1874-5997(08)00012-9

Li, Q., Lu, L. and K. Straub (2016). Storage thresholds for relative sea-level signals in the stratigraphic record. Geology., 44, 179-182. https://doi.org/10.1130/G37484.1

Machlus, M.L., Olsen, P.E., Christie-Blick, N.N., and S.R. Hemming (2008). Spectral analysis of the lower Eocene Wilkins Peak Member, Green River Formation, Wyoming: Support for Milankovitch cyclicity. Earth and Planetary Science Letters, 268, 64-75. https://doi.org/10.1016/j.epsl.2007.12.024

Malinverno, A. (1997). On the power law size distribution of turbidite beds. Basin Research, 9(4), 263-274. https://doi.org/10.1046/j.1365-2117.1997.00044.x

Maxbauer, D.P., Feinberg, J.M., Fox, D.L., and W.C. Clyde (2016). Magnetic minerals as recorders of weathering, diagenesis, and paleoclimate: a core-outcrop comparison of Paleocene-Eocene paleosols in the Bighorn Basin, WY, U.S.A. Earth Plan. Sci. Lett., 452, 15–26. https://doi.org/10.1016/j.epsl.2016.07.029

McInerney, F.A., and S.L. Wing (2011). The Paleocene-Eocene thermal maximum: a perturbation of carbon cycle, climate, and biosphere with implications for the future.

Annu. Rev. Earth Planet. Sci., 39, 489–516. https://doi.org/10.1146/annurev-earth-040610-133431

Mohrig, D., Heller, P.L., Paola, C., and W.J. Lyons (2000). Interpreting avulsion process from ancient alluvial sequences: Guadalope-Matarranya system (northern Spain) and Wasatch Formation (western Colorado). Geological Society of America Bulletin. 112(12), 1787-1803. https://doi.org/10.1130/0016-7606(2000)112<1787:IAPFAA>2.0.CO;2

Murphy, B.H., Farley, K.A., and J.C. Zachos (2010). An extraterrestrial $^{3}$He-based timescale for the Paleocene-Eocene Thermal Maximum (PETM) from Walvis Ridge, IODP Site 1266. Geochim. Cosmochim, Acta, 74, 5098–5108. https://doi.org/10.1016/j.gca.2010.03.039

Muto, T. and R.J. Steel (2001). Autostepping during the transgressive growth of deltas: results from flume experiments. Geology, 29(9), 771-774. https://doi.org/10.1130/0091-7613(2001)029<0771:ADTTGO>2.0.CO;2

Muto, T. and R.J. Steel (2004). Autogenic response of fluvial deltas to steady sea-level fall: Implications from flume-tank experiments. Geology, 32(5), 401-404. https://doi.org/10.1130/G20269.1

Myrow, P.M., Jerolmack, D.J., and J.T. Perron (2018). Bedform Disequilibrium. Journal of Sedimentary Research, 88(9), 1096–1113. https://doi.org/10.2110/jsr.2018.55

Nichols, G. (2009). Sedimentology and Stratigraphy. Blackwell Science Ltd., London, 335 p.

Olsen, P.E., Kent, D.V., Cornet, B., White, W.K., and R.W. Schlische (1996). High-resolution stratigraphy of the Newark right basin (early Mesozoic, eastern North America). Geological Society of America Bulletin, 108, 40-77. https://doi.org/10.1130/0016-7606(1996)108<0040:HRSOTN>2.3.CO;2

Paola, C. (2000). Quantitative models of sedimentary basin filling. Sedimentology, 47, 121-178. https://doi.org/10.1046/j.1365-3091.2000.00006.x

Paola, C. and L. Borgman (1991). Reconstructing random topography from preserved stratification. Sedimentology, 38(4), 553–565. https://doi.org/10.1111/j.1365-3091.1991.tb01008.x

Paola, C., and J Martin (2012). Mass-balance effects in depositional systems. Journal of Sedimentary Research, 82, 435–450. https://doi.org/10.2110/jsr.2012.38

Paola, C., Mullins, J., Ellis, C., Mohrig, D.C., Swenson, J.B., Parker, G.S., Hickson, T., Heller, P.L., Pratson, L., Syvitski, J., Sheets, B. and N. Strong (2001). Experimental Stratigraphy. GSA Today, 4-9. https://doi.org/10.1130/1052-5173(2001)011<0004:ES>2.0.CO;2

Paola, C., Parker, G., Seal, R., Sinha, S.K., Southard, J.B., and P.R. Wilcock (1992). Downstream fining by selective deposition in a laboratory flume. Science, 258(5089), 1757-1760. https://doi.org/10.1126/science.258.5089.1757

Paola, C., Straub, K.M., Mohrig, D., and L. Reinhardt (2009). The "unreasonable effectiveness" of stratigraphic and geomorphic experiments. Earth Sci. Rev., 97, 1–43. https://doi.org/10.1016/j.earscirev.2009.05.003

Pruess, K. and J. Garcıa (2002). Multiphase flow dynamics during CO2 disposal into saline aquifers. Environ. Geol., 42(2–3), 282–295. https://doi.org/10.1007/s00254-001-0498-3

Rogers, R.R. (1998). Sequence analysis of the Upper Cretaceous Two Medicine and Judith River formations, Montana; nonmarine response to the Claggett and Bearpaw marine cycles. Journal of Sedimentary Research, 68(4), 615–631. https://doi.org/10.2110/jsr.68.604

Ronayne, M.J., Gorelick, S.M., and C. Zheng (2010). Geological modeling of submeter scale heterogeneity and its influence on tracer transport in a fluvial aquifer. Water Resources Research, 46. https://doi.org/10.1029/2010WR009348

Rothman, D. H. and J.P. Grotzinger (1995). Scaling properties of gravity-driven sediments. Non-linear Processes in Geophysics, 2, 178-185. https://doi.org/10.5194/npg-2-178-1995

Rothman D.H., Grotzinger J.P., and P. Flemings (1994). Scaling in turbidite deposition, Journal of Sedimentary Research, 64, 59-67. https://doi.org/10.1306/D4267D07-2B26-11D7-8648000102C1865D

Salter, T. (1993). Fluvial scour and incision: models for their influence on the development of realistic reservoir geometries. In: North, C.P., Posser, D.J. (Eds.), Charaterisation of Fluvial and Aeolian Reservoirs. Geological Society of London Special Publication, 73, 33- 51. https://doi.org/10.1144/GSL.SP.1993.073.01.04

Secord, R., Gingerich, P.D., Smith, M.E., Clyde, W.C., Wilf, P., and B.S. Singer (2006). Geochronology and mammalian biostratigraphy of middle and upper Paleocene continental strata, Bighorn Basin, Wyoming. Am. J. Sci., 306, 211–245. https://doi.org/10.2475/ajs.306.4.211

Sheets, B.A., Hickson, T. A. , and C. Paola (2002). Assembling the stratigraphic record: Depositional patterns and time-scales in an experimental alluvial basin. Basin Res., 14, 287–301. https://doi.org/10.1046/j.1365-2117.2002.00185.x

Schulz, M., and M. Mudelsee (2002). REDFIT: estimating red-noise spectra directly from unevenly spaced paleoclimatic time series. Computers & Geosciences, 28, 421-426. https://doi.org/10.1016/S0098-3004(01)00044-9

Sloss, L.L. (1962). Stratigraphic models in exploration. Am. Assoc. Petroleum Geologists Bull, v. 46,1050-1057. https://doi.org/10.1306/74D70CD6-2B21-11D7-8648000102C1865D

Smith, F.A., Wing, S.L., and K.H. Freeman (2007). Magnitude of the carbon isotope excursion at the Paleocene-Eocene Thermal Maximum: the role of plant community change. Earth Planet. Sci. Lett., 262, 50–65. https://doi.org/10.1016/j.epsl.2007.07.021

Snell, K.E., Thrasher, B.L., Eiler, J.M., Koch, P.L., Sloan, L.C., and N.J. Tabor (2013). Hot summers in the Bighorn Basin during the early Paleogene. Geology, 41, 55–58. https://doi.org/10.1130/G33567.1

Stack, K.M., Grotzinger, J.P., and R.E. Milliken (2013). Bed Thickness Distributions on Mars: An Orbital Perspective. J. Geophys. Res., 118(6), 1323-1349. https://doi.org/10.1002/jgre.20092

Straub, K. M., Duller, R. A., Foreman, B. Z. and E.A. Hajek (2020). Buffered, incomplete, and shredded: the challenges of reading an imperfect stratigraphic record. J. Geophys. Res. Earth Surf., 125. https://doi.org/10.1029/2019JF005079

Straub, K. M., and C. R. Esposito (2013). Influence of water and sediment supply on the stratigraphic record of alluvial fans and deltas: Process controls on stratigraphic completeness. J. Geophys. Res. 118, 625–637. https://doi.org/10.1002/jgrf.20061

Straub, K. M., and B.Z. Foreman (2018). Geomorphic stasis and spatiotemporal scales of stratigraphic completeness. Geology, 46(4), 311– 314. https://doi.org/10.1130/G40045.1

Straub, K. M., Ganti, V., Paola, C., and E. Foufoula-Georgiou (2012). Prevalence of exponential bed thickness distributions in the stratigraphic record: Experiments and theory. Journal of Geophysical Research: Earth Surface, 117(F2). https://doi.org/10.1029/2011JF002034

Straub, K. M., Paola, C., Mohrig, D., Wolinsky, M. A. and T. George (2009). Compensational stacking of channelized sedimentary deposits. J. Sediment. Res., 79, 673–688. https://doi.org/10.2110/jsr.2009.070

Straub, K.M., and Y. Wang (2013). Influence of water and sediment supply on the long-term evolution of alluvial fans and deltas: Statistical characterization of basin-filling sedimentation patterns. J. Geophys. Res., 118, 1602–1616. https://doi.org/10.1002/jgrf.20095

Talling, P.J. (2001). On the frequency distribution of turbidite thickness. Sedimentology, 48, 1297–1329. https://doi.org/10.1046/j.1365-3091.2001.00423.x

Trampush, S. M. and E.A. Hajek (2017). Preserving proxy records in dynamic landscapes: modeling and examples from the Paleocene–Eocene Thermal Maximum. Geology, 45, 967–970. https://doi.org/10.1130/G39367.1

Trampush, S.M., Hajek, E.A., Straub, K.M., and E.P. Chamberlain (2017). Identifying autogenic sedimentation in fluvial-deltaic stratigraphy: Evaluating the effect of outcrop-quality data on the compensation statistic. J. Geophys. Res., 122, 91–113. https://doi.org/10.1002/2016JF004067

Tyler, N., and R.J. Finley (1991). Architectural controls on the recovery of hydrocarbons from sandstone reservoirs. Concepts in Sedimentology and Paleontology, v. 3, 1-5. https://doi.org/10.2110/csp.91.03.0001

Walcott, R.I. (1970). Flexural rigidity, thickness, and viscosity of the lithosphere. Journal of Geophysical Research, 75, 3941– 3954. https://doi.org/10.1029/jb075i020p03941

Wang, Y., Straub, K.M., and E.A. Hajek (2011). Scale-dependent compensational stacking: An estimate of autogenic time scales in channelized sedimentary deposits. Geology, 39, 811–814. https://doi.org/10.1130/G32068.1

Westerhold, T., Röhl, U., Laskar, J., Raffi, L., Bowles, J., Lourens, L.J., and J.C. Zachos (2007). On the duration of mangetochrons C24r and C25n, and the timing of early Eocene global warming events: Implications from the ODP Leg 208 Walvis Ridge depth transect. Paleoceanography, 22, PA2201. https://doi.org/10.1029/2006PA001322

Westerhold, T., Röhl, U., Wilkens, R.H., Gingerich, P.D., Clyde, W.C., Wing, S.L., Bowen, G.J. and M.J. Kraus (2018). Synchronizing early Eocene deep-sea and continental records –

cyclostratigraphic age models for the Bighorn Basin Coring Project drill cores. Climate of the Past, 14(3), 303-319. https://doi.org/10.5194/cp-14-303-2018

Wing, S.L., Harrington, G.J., Smith, F.A., Bloch, J.I., Boyer, D.M., and K.H. Freeman (2005). Transient floral change and rapid global warming at the Paleocene-Eocene boundary. Science, 310, 993–996. https://doi.org/10.1126/science.1116913

Wu, C., Nittrouer, J.A., Swanson, T., Ma, H., Barefoot, E., Best, J., and A. Mead (2020). Dune-scale cross-strata across the fluvial-deltaic backwater regime: Preservation potential of an autogenic stratigraphic signature. Geology, 48(12), 1144–1148. https://doi.org/10.1130/G47601.1

Xie, X. and P.L. Heller (2009). Plate tectonics and basin subsidence history. GSA Bulletin, 121(1-2), 55–64. https://doi.org/10.1130/B26398.1

Zachos, J.C., Pagani, M., Sloan, L., Thomas, E., and K. Billups (2001). Trends, rhythms, and aberrations in global climate 65 Ma to present. Science, 292, 686–693. https://doi.org/10.1126/science.1059412

Zachos, J.C., McCarren, H., Murphy, B., Röhl, U., and T. Westerhold (2010). Tempo and scale of late Paleocene and early Eocene carbon isotope cycles: Implications for the origin of hyperthermals. Earth Planet. Sci. Lett., 299, 242-249. https://doi.org/10.1016/j.epsl.2010.09.004

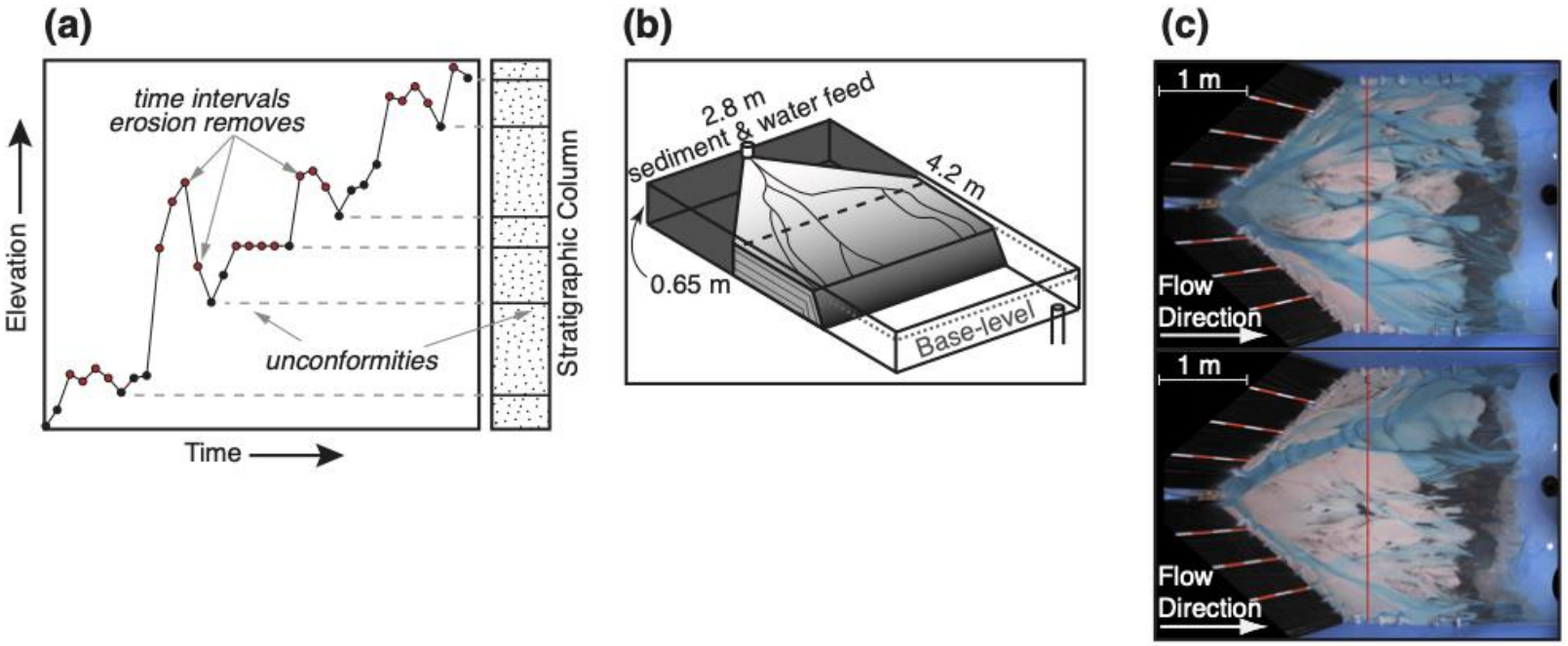


**Figure 1.** a) Schematic diagram illustrating the construction of a stratigraphic column from elevation increments. b) Schematic diagram of TDB-10-1 experimental set up with basin dimensions. c) Overhead images of TDB-10-1 experiment. Red line identifies proximal transect where 100 random samples were taken.

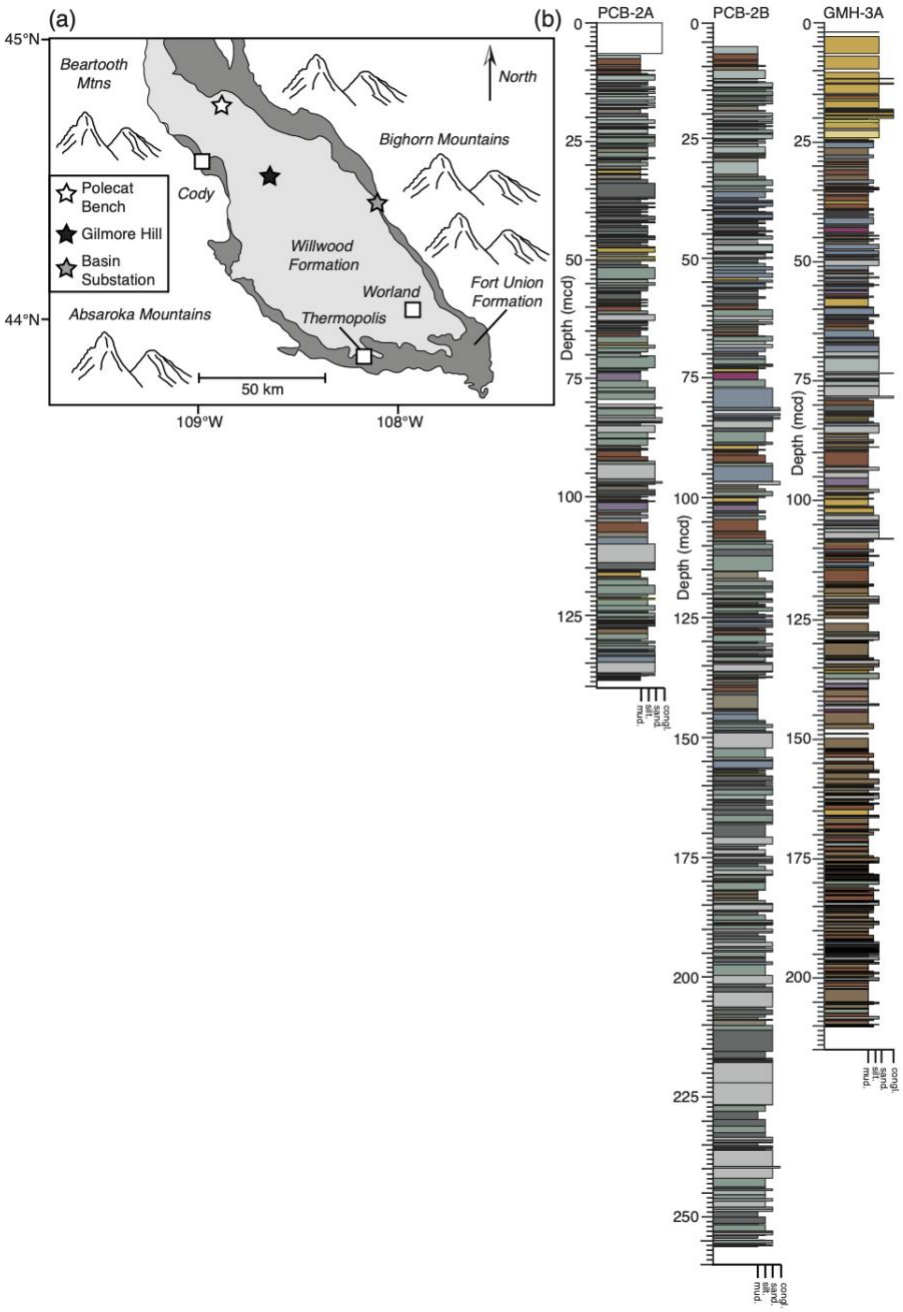


**Figure 2.** a) Map of field study area, Bighorn Basin, Wyoming. Locations of sample cores indicated with a star. b) Lithologic logs of sample cores used in quantitative analysis. Grey and yellow beds are generally crevasse splay deposits and C-horizons of paleosols. Red, orange, and purple beds are generally B-horizons of paleosols (modified from Clyde et al., 2013).

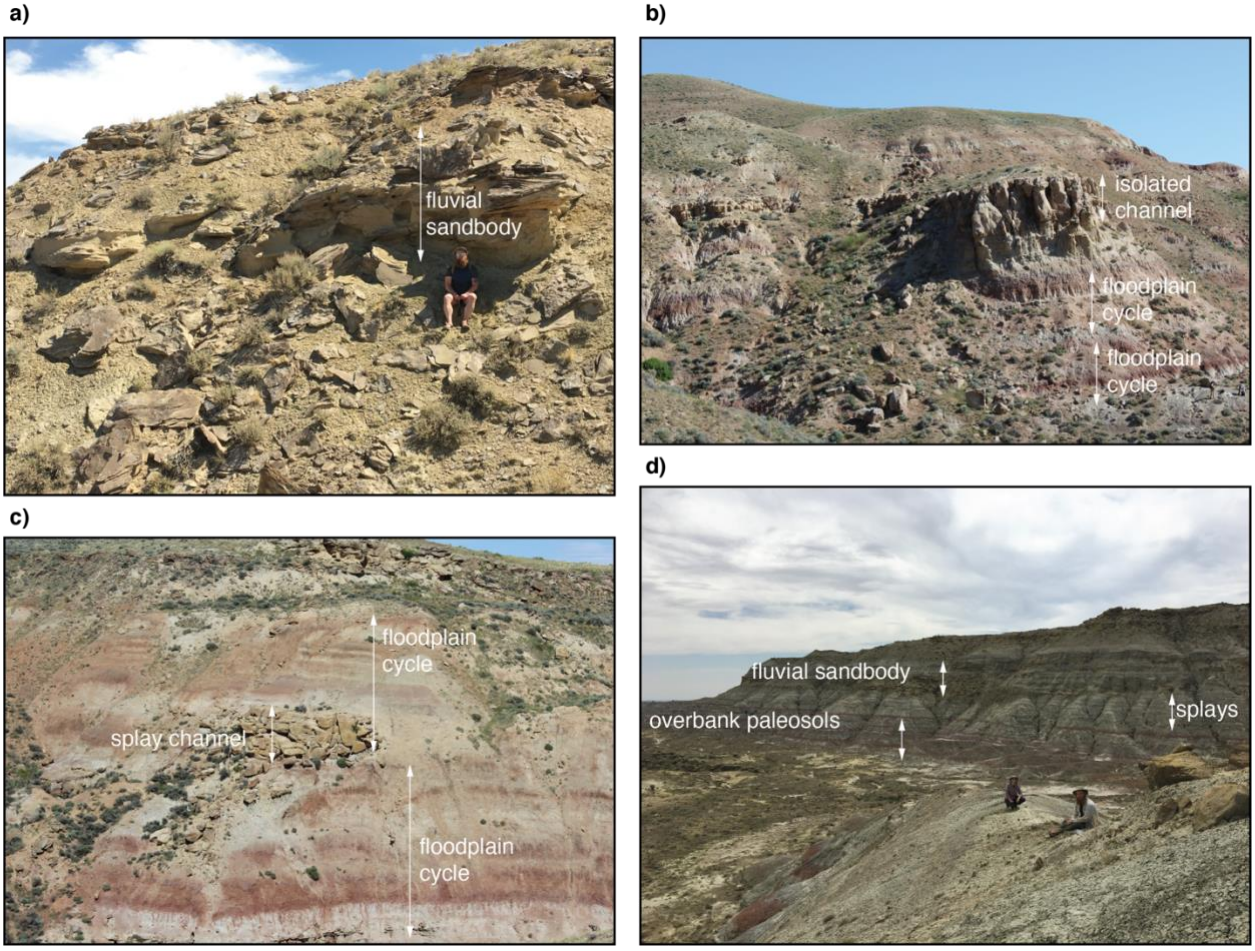


Figure 3. Annotated photographs of the Willwood Formation, Bighorn Basin, WY. a) Close up image of a fluvial sandbody with graduate student for scale. b) Fluvial sandbody deposited on top of red mudstones that signify floodplain deposits. c) Splay channel deposited in between red beds above there is a bigger, laterally continuous sandbody unit d) Overbank paleosol red beds with white-ish splay zones, fluvial sandbodies higher in section.

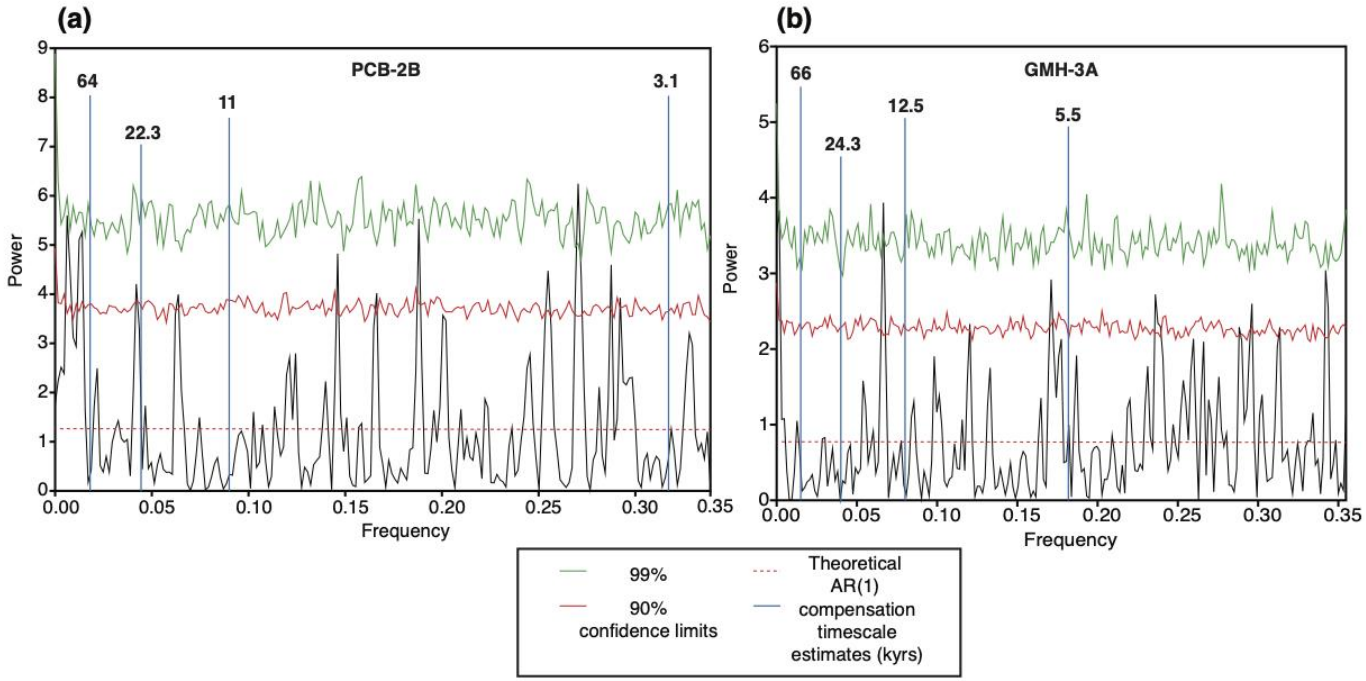


**Figure 4.** Nondimensionalized discontinuous time series plots of PCB-2B (a) and GMH-3A (b) including estimated compensation timescales.

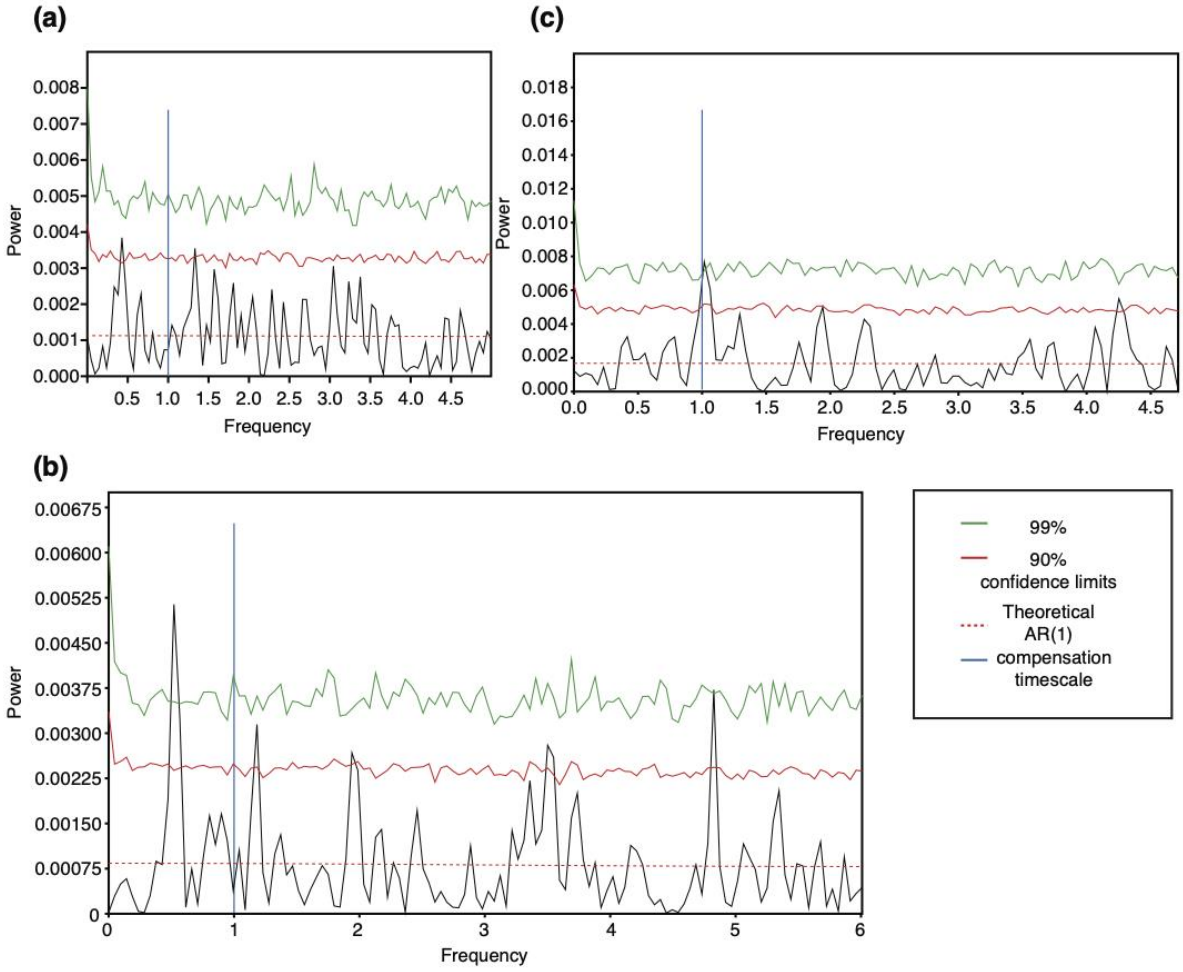


**Figure 5.** Nondimensionalized discontinuous time series plots for TDB-10-1. a) Plot with no statistically significant cycles. b) Plot with a cycle near the compensation timescale. c) Plot with statistically significant cycles both shorter and longer than the compensation timescale.

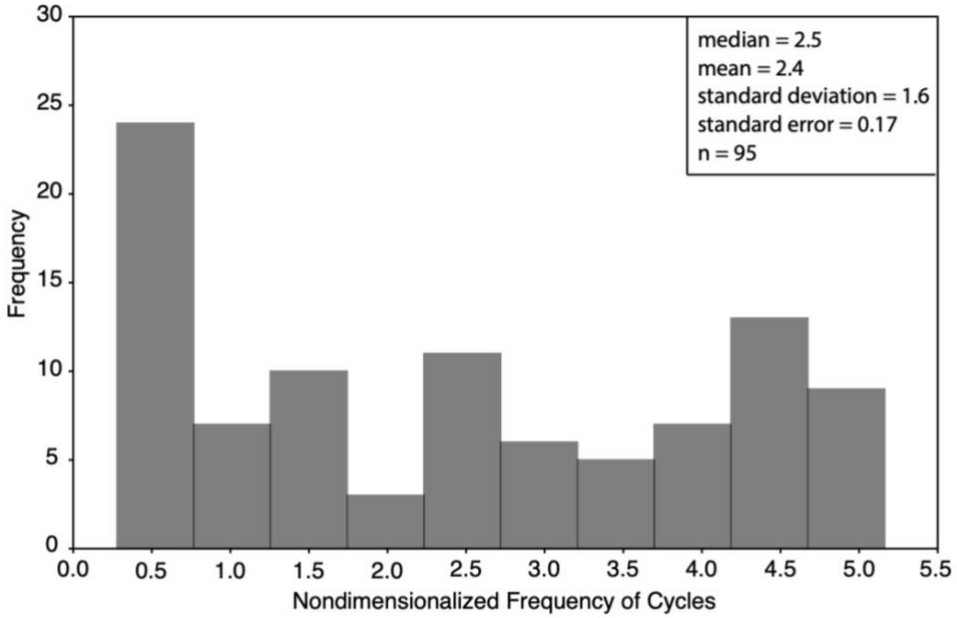


**Figure 6.** Histogram of nondimensionalized cycle frequencies from TDB-10-1.

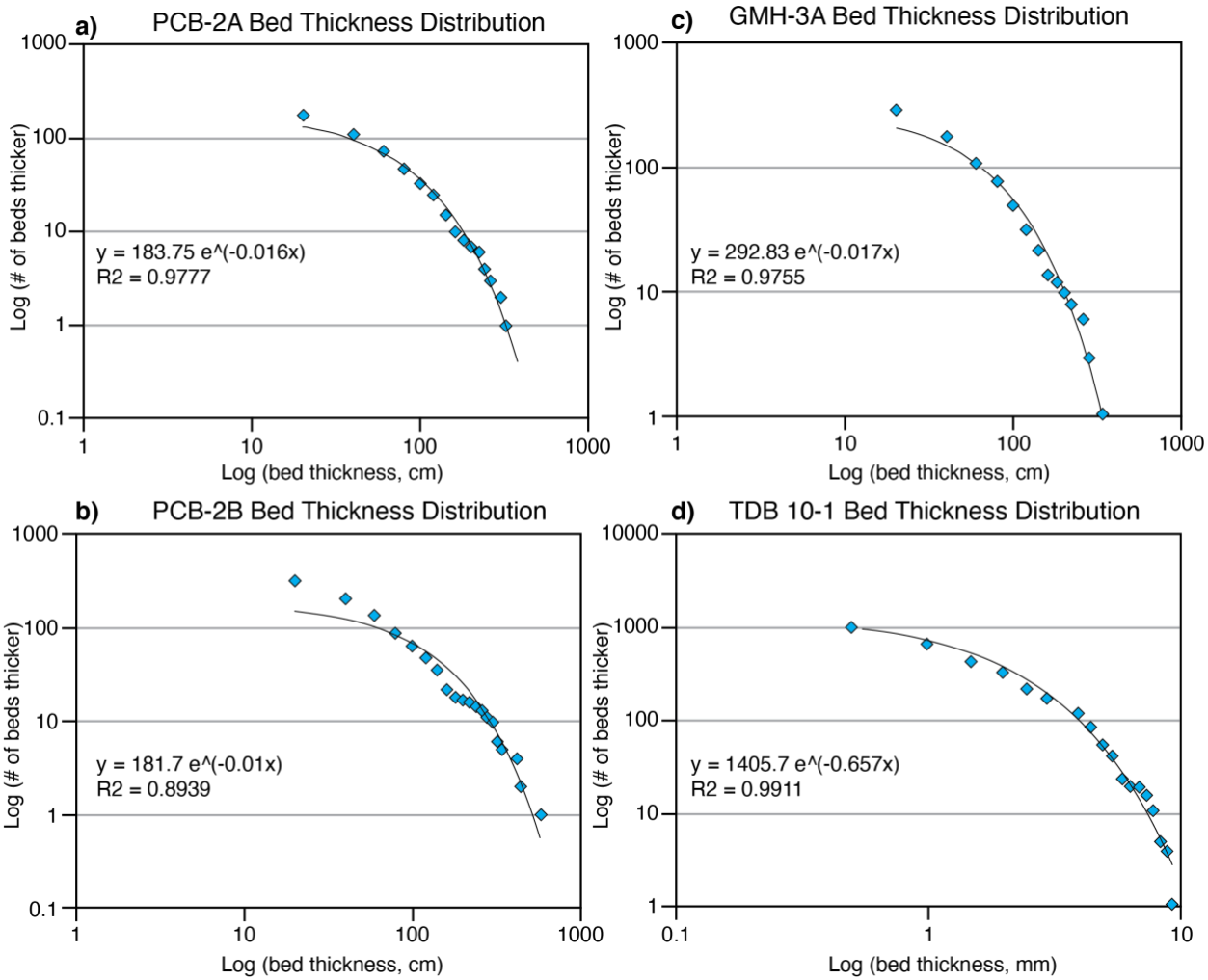


**Figure 7.** Log-log plots of bed thickness distributions (a) PCB-2A (b) GMH-3A (c) PCB-2B (d) TDB-10-1 including regression line with coefficient of determination.

| TDB-10-1 Location Sample Number | Nondimensionalized Frequency | TDB-10-1 Location Sample Number | Nondimensionalized Frequency | TDB-10-1 Location Sample Number | Nondimensionalized Frequency |
|---|---|---|---|---|---|
| 227 | 0.52045 | 695 | 2.4909 | 1333 | 0.65197 |
| | 4.826 | | 4.7938 | | 3.4927 |
| 234 | no cycles | 753 | no cycles | 1348 | no cycles |
| 243 | 0.52033 | 756 | no cycles | 1356 | no cycles |
| | 2.4125 | 787 | 1.0167 | 1381 | 4.54420 |
| | 3.5477 | 794 | 2.8407 | 1398 | 4.21480 |
| 265 | 1.46440 | 813 | 2.7691 | 1429 | no cycles |
| | 4.724 | 822 | 1.44170 | 1451 | 0.56311 |
| 267 | 4.86960 | | 2.4648 | | 1.7363 |
| 277 | 2.7785 | 869 | no cycles | 1480 | 2.67890 |
| | 4.6622 | 907 | no cycles | | 4.0419 |
| | 4.8506 | 915 | 3.1629 | 1500 | 4.24210 |
| 317 | 4.8792 | 921 | 1.725 | 1552 | no cycles |
| 347 | 4.2765 | | 3.7854 | 1561 | 4.34210 |
| 357 | 3.0885 | 926 | 1.7196 | 1566 | no cycles |
| | 4.2764 | | 2.054 | 1583 | 2.56770 |
| 375 | no cycles | | 2.6271 | 1584 | 2.56750 |
| 388 | no cycles | | 4.3945 | 1592 | 0.42800 |
| 418 | 4.15780 | 949 | 4.4779 | 1598 | no cycles |
| 429 | 0.38297 | 1040 | no cycles | 1604 | no cycles |
| | 1.4361 | 1054 | 0.82835 | 1607 | 2.89680 |
| 436 | 0.38406 | | 2.485 | 1612 | no cycles |
| | 0.81613 | | 4.0037 | 1661 | 0.56726 |
| | 1.4402 | 1081 | no cycles | 1673 | 0.56641 |
| 452 | 0.3382 | 1082 | no cycles | 1683 | 0.56559 |
| | 1.4494 | 1094 | 0.5507 | 1695 | 3.95240 |
| | 4.2517 | 1123 | no cycles | 1703 | 0.51527 |
| 466 | 0.38762 | 1147 | no cycles | 1705 | no cycles |
| | 1.4513 | 1175 | no cycles | 1721 | 0.56218 |
| | 4.3539 | 1178 | 2.1663 | 1723 | no cycles |
| 492 | no cycles | 1211 | 3.9801 | 1766 | 2.58500 |
| 520 | no cycles | 1225 | 1.7584 | 1768 | 4.17670 |
| 532 | no cycles | | 2.591 | 1786 | 4.82530 |
| 544 | 5.1621 | 1250 | 0.27766 | 1789 | no cycles |
| 564 | 0.28935 | 1252 | 0.27883 | 1790 | 4.82690 |
| 566 | 0.28981 | 1293 | 0.97782 | 1821 | no cycles |
| 579 | 0.6259 | | 3.3991 | 1834 | 4.57350 |
| 581 | 0.62581 | 1298 | 0.93160 | 1837 | no cycles |
| 598 | 0.28578 | 1307 | 1.49290 | 1868 | no cycles |
| | 2.572 | 1310 | 0.51313 | 1881 | 3.37870 |
| 631 | no cycles | | 0.93296 | 1887 | 4.49200 |
| 658 | no cycles | 1324 | 0.79532 | | |
| 663 | no cycles | | 3.5088 | | |
| 675 | 0.28196 | | | | |

Table 1. Data table of TDB-10-1 experimental bed thickness frequencies.

| Location | Linear Equation | R-squared | Logarithmic Equation | R-squared | Exponential Equation | R-squared | Power Law Equation | R-squared |
|---|---|---|---|---|---|---|---|---|
| PCB-2A | -0.4318x + 105.65 | 0.6152 | -62.09ln(x) + 337.45 | 0.9078 | 183.75e^(-0.016x) | 0.9777 | 107733x^(-1.85) | 0.8589 |
| PCB-2B | -0.38x + 137.85 | 0.4477 | -89.28ln(x) + 511.81 | 0.839 | 181.7e^(-0.01x) | 0.8939 | 126703x^(-1.709) | 0.8736 |
| GMH-3A | -0.6796x + 165.51 | 0.5782 | -100.4ln(x) + 542.62 | 0.8939 | 292.83e^(-0.017x) | 0.9755 | 215191x^(-1.913) | 0.8616 |
| TDB 10-1 | -79.113x + 585.93 | 0.6471 | -326.7ln(x) + 636.08 | 0.9232 | 1405.7e^(-0.657x) | 0.9911 | 911.32x^(-2.1) | 0.7817 |

**Table 2.** Data table of trendline equations and r-squared values for each distribution chart.

Best fit R-squared values are highlighted in yellow.